Environmental Modelling and Software 204 (2026) 107065

Contents lists available at ScienceDirect

Environmental Modelling and Software

journal homepage: www.elsevier.com/locate/envsoft

Towards precision irrigation scheduling from UAV-based observations: Model structure

Meng Cao [a,*], Jeffrey P. Walker [a], Xiaoling Wu [a], Mostafa Rahimi Jamnani [a], John D. Bussell [b], Ivor Gaylard [b], James Hills [c]

[a] Department of Civil and Environmental Engineering, Monash University, Clayton, Australia
[b] SWAN Systems, Perth, Australia
[c] Tasmanian Institute of Agriculture, Livestock Production Centre, The University of Tasmania, Burnie, Tasmania, Australia

ARTICLE INFO

Keywords:
Soil moisture
Conceptual soil moisture model
Buckingham-Darcy equation
Evapotranspiration
Precision irrigation

ABSTRACT

Using UAV-based near-surface observations for root-zone soil moisture (RZSM) estimation requires a model with at least two layers and minimal complexity while this design has been overlooked. To address this limitation, a series of soil moisture models, from two-layer to multi-layer configurations were developed. Key processes, including vertical soil moisture redistribution, evapotranspiration, drainage, and infiltration, were progressively refined and systematically evaluated. A two-layer model incorporating Buckingham Darcy based vertical fluxes and a water stress adjusted evapotranspiration scheme (R-FLX-ET) was identified as the optimal configuration, achieving high accuracy with limited complexity. The R-FLX-ET model produced NSE up to 0.92 for RZSM and 0.81 for near surface soil moisture at hourly resolution, with RMSE below 0.03 cm^3 cm^{-3}, outperforming both the single-layer model and Aqua Crop. Model robustness was confirmed through numerical stability analysis and validation across four monitoring stations. R-FLX-ET offers a computationally efficient framework suitable for UAV-assisted precision irrigation applications.

1. Introduction

Irrigation water use is essential for global crop production and accounts for nearly 90% of consumptive water use (Global Land Evaporation Amsterdam Model; Han et al., 2020; Scanlon et al., 2012). When faced with water shortage due to global population growth, the need to enhance irrigation efficiency becomes increasingly important. Precision irrigation, delivering only the required amount of water at optimal times and locations, can improve water use efficiency by 15-35% compared with conventional methods such as center-pivot irrigation (Pan et al., 2015).

There are two main categories of irrigation scheduling, defined as soil moisture based and plant condition based (Jones, 2004). Although irrigation water application is directly related to vegetation conditions, making plant condition-based methods possibly more accurate, challenges in measuring plant water stress makes these methods difficult to implement (Jones, 2004; Pan et al., 2015). Moreover, there is a time latency between soil moisture conditions and crop conditions, meaning actions may be too late by the time that crop water stress can be observed (Rekika et al., 2014). Conversely, irrigation scheduling based on soil moisture conditions can directly provide the amount of water needed to be applied for optimal conditions, enabling forecasts for planning an appropriate irrigation schedule and reducing the impact of meteorological factors (Wu et al., 2023; Xu et al., 2021b; Yu et al., 2021).

The root zone soil moisture (RZSM) directly controls plant nutrients and water uptake, making it a critical component in ensuring optimum agricultural productivity (Baldwin et al., 2017; Sahaar et al., 2020; Seneviratne et al., 2012). Therefore, adequate knowledge of moisture dynamics in deeper soil layers is an important indicator of irrigation scheduling requirements. At the farm scale, RZSM can be determined through two different approaches: (1) direct in-situ soil moisture measurement and (2) estimation based on water-balance modelling (Ahmadi et al., 2022; Kashyap and Kumar 2021; Xu et al., 2021c). The in-situ farm scale RZSM measurements can be collected by either gravimetric methods or installing soil moisture measurement sensors (Bogena et al., 2007). However, they have the problem of extrapolating the measured values due to inhomogeneities such as soil texture and

* Corresponding author.
E-mail address: meng.cao@monash.edu (M. Cao).

https://doi.org/10.1016/j.envsoft.2026.107065
Received 16 December 2025; Received in revised form 13 May 2026; Accepted 2 June 2026
Available online 6 June 2026

micro-topography (Hu et al., 2017; Wigmore et al., 2019; Xu et al., 2018), in addition to the expense of materials and labor. Conversely, soil moisture models based on water-balance calculations provide a method of directly estimating spatial variation in RZSM with a fine spatial resolution for precision irrigation (Hirschi et al., 2014; Khandan et al., 2022; Kumar et al., 2013), but are prone to errors due to simplified model physics, poor estimates of soil hydraulic parameters, and inaccurate weather data (Ahmadi et al., 2022; Rouf et al., 2021; Walker et al. 2001a, 2001b).

Utilizing near-surface soil moisture information in the physical models, either in calibrating soil hydraulic parameters or through assimilation to update the model states, is one way to enhance the simulation accuracy. Such methods have been applied to satellite data (Baldwin et al., 2017; Hirschi et al., 2014; Rouf et al., 2021; Xu et al., 2025), with several soil moisture products available publicly, including GLDAS (Global Land Data Assimilation System), MERRA2 (Modern-Era Retrospective Analysis for Research and Applications, Version 2), NLDAS (North American Land Data Assimilation System), NCEP (National Centers for Environmental Prediction) and JRA (Japanese Year Reanalysis)-55 (Ojha et al., 2024; Pablos et al., 2018; Xu et al., 2021c). However, studies have rarely been conducted at the farm scale, due to the coarse spatial resolution of satellite soil moisture products and lack of an appropriate high spatial resolution soil moisture model (Ahmadi et al., 2022). Geng et al. (2025) proposed a new algorithm for soil moisture estimation based on land surface temperature, providing the possibility of mapping near-surface soil moisture at finer spatial resolutions (~2 km). However, it might still be inadequate for farm-scale applications. The development of advanced Uncrewed Aerial Vehicles (UAVs) offers a platform that can be equipped with a microwave radiometer to deliver higher-resolution imagery at tens of meters for estimating near-surface soil moisture at sub-field scale, but a suitable soil moisture model needs to be developed coupling with this UAV-based near-surface information in order to provide RZSM estimates (Vianna et al., 2024).

The soil moisture models currently applied in precision irrigation and incorporated into irrigation software are typically simple “bucket” models, being lumped models that conceptualize a single soil layer over the rooting depth as a bucket that receives and retains all incident water until its capacity is filled, ignoring some physical processes and thus not representing real-world conditions (Baldwin et al., 2017; Li et al., 2025). Such models consider the soil layer receiving and retaining all incident water until its capacity is filled, while ignoring soil water redistribution and the feedback between soil water storage and evapotranspiration (Aboitiz et al., 1986; Guswa et al., 2002; Romano et al., 2011). Additionally, a model with at least two layers is required, with a root zone layer and a near-surface layer that can be matched to the UAV-based near-surface soil moisture observations for improving the RZSM estimation accuracy (Walker et al., 2001a). While the land surface models (LSM) commonly used in coupling with remote sensing based observations provide detailed information throughout the whole soil profile, their algorithms are typically complex, making them difficult to implement at farm-scale due to their requirements for detailed model inputs and having a low computational efficiency (Jarvis et al., 2022; Sahoo and Liu, 2022; Xu et al., 2021a). While soil moisture models applied in agriculture are generally gross simplifications of reality, some components require careful and detailed representation to ensure accuracy of the soil moisture dynamics. Thus, necessary simplification without compromising the model accuracy must be addressed to enhance their usefulness, especially when utilizing calibration and data assimilation approaches based on near-surface soil moisture observation constraint.

A full understanding of which components can be simplified in RZSM estimation models to capture the necessary dynamics of soil moisture has not been systematically examined, especially in the context of precision irrigation. Even though several soil moisture models utilized in agricultural contexts have been compared, the role of each model component on simulation accuracy has not been addressed (Vianna et al., 2024). Therefore, this study has investigated the impact of each component of the soil moisture model, examining the necessity of increasing model complexity and providing a model base for the calibration and/or assimilation of UAV-based near-surface soil moisture. In this context, UAV-based observations are considered as a key design constraint for model development, as they only provide near-surface soil moisture information, requiring an explicit representation of the near-surface layer (e.g., ~5 cm), and are expected to be temporally sparse due to practical flight limitations. These characteristics necessitate a model structure that contains at least two soil layers, remains sufficiently simple for practical application of estimating the temporal evolution of soil moisture, and is capable of reliably propagating near-surface soil moisture observations to the root-zone. In this study, soil moisture models with increasing complexity were developed based on a single bucket model framework. Soil moisture simulations (both near-surface and root zone) were compared to balance the model accuracy and simplicity. A series of two-layer models with different components were developed and compared against each other as well as against *in-situ* data and output from a well-established soil moisture model used in agriculture. Multi-layer models were then developed to examine the impact of soil horizons and horizon discretization based on the selected two-layer model structure. Ultimately, the objective of this study was to develop a suitable soil moisture model with the least complexity to achieve the utilization of UAV-based near-surface soil moisture observations to improve RZSM estimates.

2. Materials and methods

2.1. Study area

The study area was a ~400 m diameter center pivot irrigation site within the Newry area (referred to simply as Newry hereafter; 146°51′19″E to 146°51′46″E and 37°54′14″S to 37°54′38″S, Fig. 1), located in central Gippsland, southeastern Victoria, Australia. With 28% of the region's land dedicated to agricultural use, Gippsland farms produce 28.6% of the dairy and 19% of the vegetable produce for Victoria, making agricultural plans for this area vitally important to ensuring the sustainability of food production (McDonald et al., 2024). Being within the Temperate Oceanic Climate (Cfb) zone, the annual precipitation for Gippsland is around 500~700 mm. More specifically, the annual precipitation for the Newry site is on average 593 mm, and the average minimum and maximum temperature is 8.2°C and 19.7°C, respectively. Precipitation is almost evenly distributed throughout the year, with monthly averages ranging from 40.6 mm in February to 63.0 mm in November. Due to the strong solar radiation (around 1800 kWh/m^2/year) and wind speed (around 16-17 km/h), annual potential evapotranspiration (PET) in Newry is 1000~1400 mm/year (State Government of VictoriaM.Australia, 2024). Therefore, there is a water deficit of 300~900 mm per year, making irrigation essential for agricultural production in the area. With increased temperature and decreased precipitation according to climate predictions, an increased water deficit and higher irrigation demand is to be expected in the future (McKay et al., 2023; Rauniyar and Power, 2023).

Newry is located in a semi-arid agricultural and grazing area, with the experiment site routinely cultivated with a range of crop types including pasture, corn, oat and wheat, making it a suitable site for exploring the efficiency of soil moisture modelling and data assimilation across the different vegetation types typical of precision irrigation farms in the region. Moreover, this farm has been monitored as a core precision agriculture site by Agriculture Victoria since 2016, further highlighting its suitability for this study in terms of background knowledge, scientific requirements, and logistics.

2.2. Site description and data collection

Monitoring stations were installed within the field to provide the

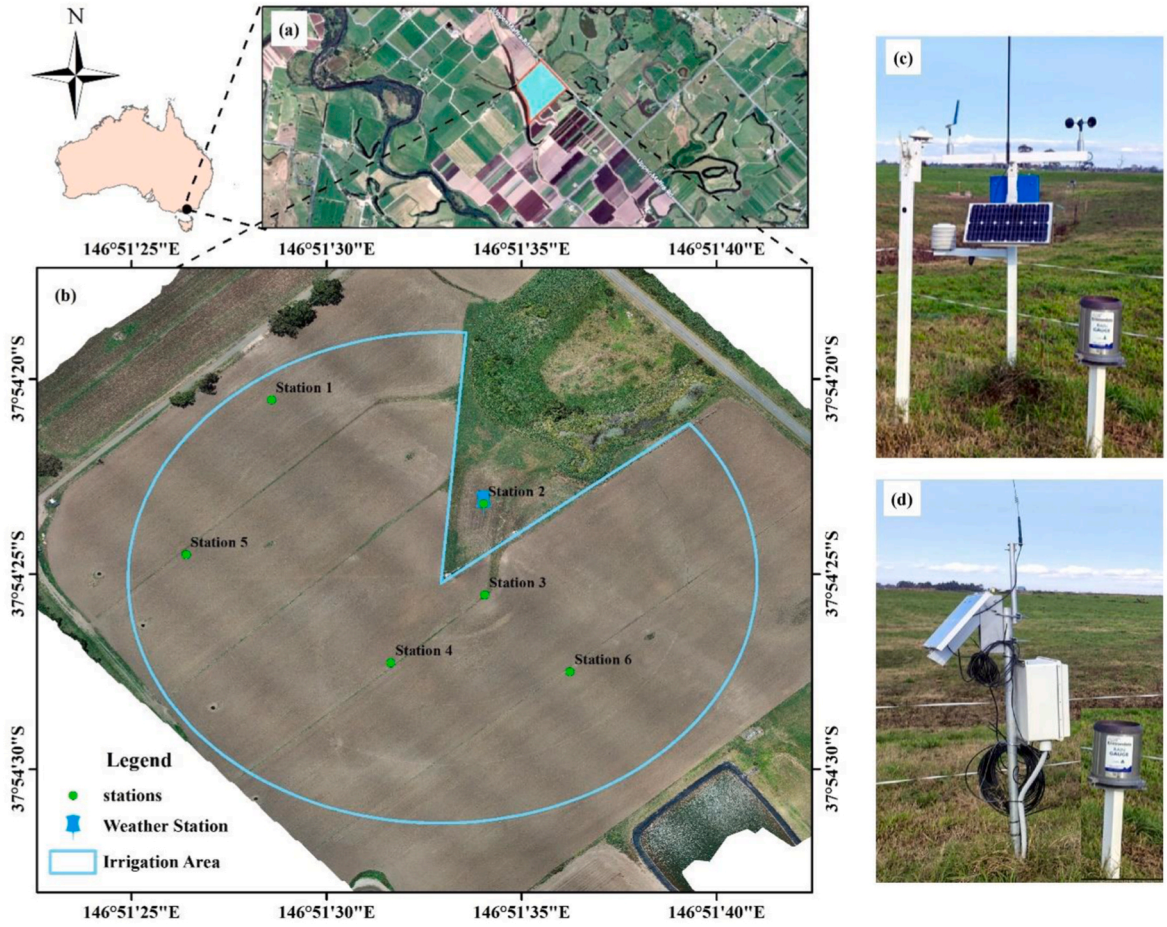

Fig. 1. Location of the study area and distribution of monitoring stations. (a) Location of the study area; (b) distribution of soil moisture and weather stations along with the irrigation area; (c) photograph of the weather station; and (d) photograph of one soil moisture station (Station 6).

data required. This included 6 soil moisture monitoring stations (Fig. 1d), providing continuous in-situ soil moisture observations. Each soil moisture station has 9 Stevens Water Hydra probes to monitor the soil water content and soil temperature, being at 5 cm increments over the top 40 cm layer, and then one at 60 cm (Figs. 1 and 2). Soil moisture recordings were regularly and carefully checked based on geometric methods. Additionally, three soil temperature sensors distributed at 1, 2.5 and 4 cm depths were installed to measure soil temperature for each station. All soil moisture, soil temperature and rainfall data were recorded with a 20 min time interval. The location of the soil moisture stations (Fig. 1 b and Table 1) was chosen utilizing soil type information based on EM38 measurements by Agriculture Victoria. The reliability of

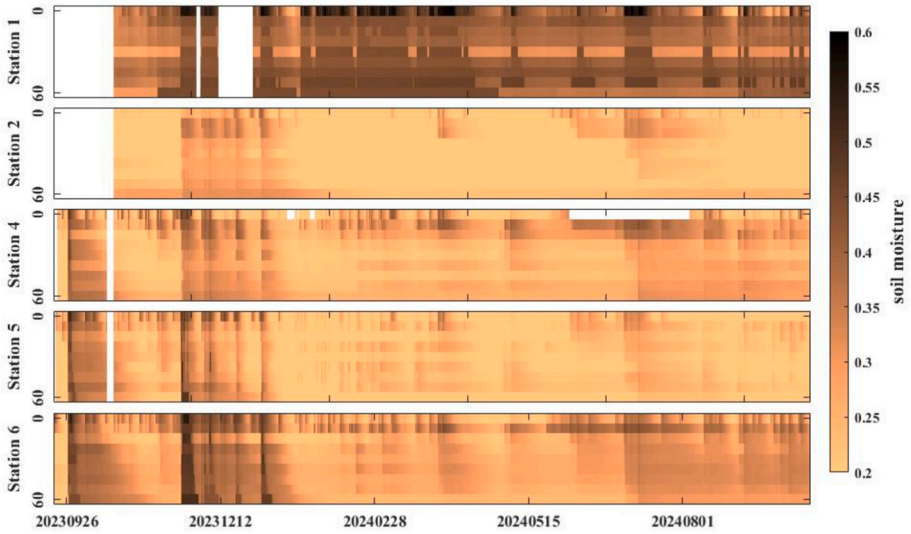

Fig. 2. Overview of valid soil moisture observations across all stations. Blank segments indicate data gaps caused by sensor malfunctions.

Table 1
Calibration and validation period for each soil moisture station.

Station	Water regime	Calibration Period	Validation Period
1	Irrigated	Discarded due to inoperable rain gauge	
2	Rainfed	2023.12.01-2024.01.31	2024.02.01-2024.10.10
3	Irrigated	Discarded due to noise in soil moisture sensor data	
4	Irrigated	2023.12.09-2024.01.26	2024.03.24-2024.05.07
5	Irrigated	2023.12.01-2024.01.26	2024.05.10-2024.10.10
6	Irrigated	2023.09.27-2023.12.26	2024.05.31-2024.10.10

soil moisture was checked according to the dynamics in response to rainfall and cross-checked between each station. Rainfall (including irrigation amount) was recorded based on a rain gauge co-located with each soil moisture station. The reliability of rain gauge data was checked by comparing to a separate weather station rain gauge and irrigation diary, and cross-checked with rain gauges installed at the soil moisture stations, as well as with stations installed by the Australian Bureau of Meteorology. A weather station (Fig. 1c) located at 146.859454°E, −37.906444°S (Fig. 1 b) was installed to provide data for calculating potential evapotranspiration, including wind speed and direction, air temperature, air humidity, solar radiation, rainfall, soil temperature, soil electrical conductivity and soil moisture every 10 min.

The management sequence applied to all monitoring stations within the irrigation area (Stations 1 and 3–6) consisted of the following treatments: (1) pasture, (2) deep ripping, (3) bare soil with sowing for corn, (4) corn crop, and (5) oat crop. Since all stations except Station 2 underwent deep ripping on 10 October 2024, only data collected prior to this date were used in the analysis presented herein. During this period the stations were under pasture, providing a stable baseline that was less affected by crop-specific influences. This ensured that the soil moisture model could be evaluated under relatively consistent natural conditions to support broader applicability across different crop seasons, and with a longer continuous data record. While crop-specific parameterization will be incorporated in later stages, the model structure will remain unchanged. Calibration and validation periods were separated on 31 January 2024, corresponding to approximately half of the total record length since the initial station installation. Data preceding this date were used for calibration while the subsequent data were used for validation, with only quality-checked observations retained, leading to station-specific period definitions (Table 1).

2.3. Model framework and revised components description

In irrigation applications, soil moisture modelling approaches generally include conceptual models (e.g., single-layer or multi-layer bucket models), physically based models (e.g., Richards' equation-based models such as HYDRUS), and crop-oriented models (e.g., Aqua Crop). Among these approaches, conceptual models are most commonly applied for soil moisture estimation due to their simplicity and low data requirements. However, the appropriate level of model complexity, including the number of components and soil layers, remains unclear. Therefore, the soil moisture modelling framework adopted in this study is based on a single-layer bucket model (hereafter referred to as the SL model), from which the minimum model complexity is systematically explored. Important model components, including soil moisture redistribution, evapotranspiration, drainage and infiltration were then revised systematically to explore their contribution to soil moisture accuracy based on a two-layer model framework. Multi-layer models with different soil horizons and vertical discretion were then discussed based on the optimal two-layer model configuration to explore the influence of model layers on the model accuracy. In this study, the concept of minimum model complexity is explicitly defined from structural, parametric, and computational perspectives. Structural complexity refers to the number of soil layers and model components, parametric complexity to the number of parameters requiring calibration, and computational complexity to the numerical scheme and associated computational cost. Accordingly, minimum model complexity is defined as the simplest model configuration that achieves satisfactory simulation performance without introducing unnecessary parameters or structural components.

2.3.1. Model framework

The model framework presented here is the description of a basic SL model framework commonly used in irrigation scheduling.

(1) Effective Rainfall

The SL model uses two parameters to control the amount of rainfall that will penetrate into the soil layer: *Rain_minpen* and *Rain_maxpen*. The value of *Rain_minpen* represents the amount of rainfall that is captured by the vegetation canopy not contributing to soil moisture, while the value of *Rain_maxpen* represents the maximum amount of rainfall that can infiltrate into the soil in a single calculation step (hour, day and etc.) due to the capacity of the soil to absorb moisture. The effective rainfall that is therefore available to increase the moisture content of the soil is the amount of rainfall within those constraints, limited by the available water storage capacity in the soil, and calculated according to

$$Rain_{effective} = \min\left[\max\left(0, Rain_{total} - Rain_{minpen}\right), \left(Rain_{maxpen} - Rain_{minpen}\right), \left(\theta_s + ETc + Drain_{prelim} - \theta_{t-1}\right)\right], \quad (1)$$

where *Rain_effective* (mm) is the amount of rainfall used in the soil moisture calculation step, *Rain_total* (mm) represents the rainfall measured by the rain gauge, θ_s means the saturation point of the soil (in terms of mm of storage) otherwise known as the porosity, *ETc* (mm) denotes the water stress adjusted evapotranspiration, and *Drain_prelim* (mm) is the drainage estimate based on the soil moisture content (θ_{t-1}; mm) from the last step.

(2) Irrigation

Irrigation in the SL model is estimated according to the amount of water that is applied to the system and the system efficiency by

$$IRRGtotal = \frac{FMvol \times 0.0001}{IRRG} \quad (2)$$

$$IRRGnet = IRRGtotal \times Efficiency \times 0.01, \quad (3)$$

where *FMvol* (ML) is the total amount of water scheduled for irrigation, *IRRGtotal* (mm) is the total amount of water that is applied in the system, *IRRGnet* (mm) denotes the amount of water delivered by the system to the ground, *IRRG* (ha) represents the area of irrigation, and *Efficiency* (%) is the efficiency of irrigation system. For this study, a rain gauge in every station provided direct measurements of both rainfall and irrigation and so this calculation was not applied. Although irrigation maps were not incorporated in this study, the irrigation equations were retained here to illustrate the general method of water application.

(3) Evapotranspiration

Evapotranspiration (*ET*) is estimated by weather station data according to the Penman-Monteith equation (Allen et al., 1996)

$$ET_0 = \frac{0.408\Delta(Rn - G) + \gamma \frac{900}{T+273} u_2 (e_s - e_a)}{\Delta + \gamma(1 + 0.34u_2)}, \quad (4)$$

in which ET_0 (mm) is the reference evaporation, Δ (kPa/°C) denotes the slope of the vapor pressure curve, R_n (MJ/m^2) is the net radiation, G (MJ/m^2) is the soil heat flux density, γ (kPa/°C) is the psychrometric constant, T (°C) is the air temperature, u_2 (m/s) denotes the wind speed at 2 m height above the ground, and e_s (kPa) and e_a (kPa) are the saturated and actual vapor pressure respectively. These variables were

calculated based on weather station-based measurements. In this study, ET_0 was calculated from daily weather forcing data and averaged to hourly resolution when the model was driven with hourly inputs, consistent with the practical availability of field observations.

(4) Drainage

Drainage in the SL model is the soil moisture in excess of its field capacity. Accordingly, it is calculated as

$$Drain\_total = Drain\_prelim + \max\left[0, \left(\theta_{prelim} - \theta_s\right)\right] \tag{5}$$

$$\theta_{prelim} = \theta_{t-1} - ETc + Rain_{effective} + IRRGnet - Drain_{prelim}, \tag{6}$$

where *Drain_total* (mm) is the total amount of drainage, and *Drain_prelim* (mm) is the drainage due to soil moisture content in excess of the field capacity in the last time step calculated as

$$Drain_{prelim} = \begin{cases} [\theta_{t-1} - \theta_{FC}] \times Drain_{coff} & \theta_{t-1} > \theta_{FC} \\ 0 \quad \theta_{t-1} \le \theta_{FC} \end{cases}, \tag{7}$$

where θ_{t-1} (mm) is the soil moisture in the last time step, and *Drain_coff* is a drainage coefficient defined by model calibration.

(5) Soil Moisture

The soil moisture content is finally estimated from the inputs and outputs described above according to

$$\theta(t) = \theta(t-1) + Rain_{effective} + \frac{IRRI_{net}}{wetarea(\%) \times 0.01} - \frac{ETc}{wetarea(\%) \times 0.01} - Drain_{total}, \tag{8}$$

where θ (mm) is the soil moisture content and *wetarea* denotes the percentage of area irrigated.

2.3.2. Revised model components

To determine the optimal model configuration, a series of two-layer soil moisture models (the foundation of near-surface soil moisture data assimilation and/or calibration), with additional and/or alternative component concepts were used to provide the soil moisture estimates. Accordingly, each model component was revised incrementally to see its effect and to maintain a minimum level of model complexity. Components which yielded noticeable improvements in soil moisture simulation were retained, while those with limited contribution were excluded from further analysis. All revised equations were formulated based on the requirement of at least a two-layer structure, and the algorithms for the retained components designed to be extendable to multi-layer configurations. The differences between soil moisture models with different components are summarized in Table 2.

(1) Soil moisture redistribution

The Buckingham-Darcy equation was applied for calculating the vertical soil moisture redistribution flux between soil layers according to

$$q = K_\theta \left[\frac{\Psi_{m,j} - \Psi_{m,j+1}}{1/2 \times \left(d_j + d_{j+1}\right)}\right] + K_\theta, \tag{9}$$

where q (mm/h) denotes the soil moisture vertical flux between layer j and layer $j+1$, with positive values indicating downward flow, K_θ (mm/h) is the unsaturated hydraulic conductivity, d_j and d_{j+1} represent the soil thicknesses (mm) of the two layers, $\Psi_{m,j} - \Psi_{m,j+1}$ is the difference in matric potential (mm) between the two layers, derived by the van Genuchten (Vangenuchten, 1980) equation

$$\theta(h) = \theta_r + \frac{\theta_s - \theta_r}{\left[1 + (\alpha|h|)^n\right]^m}, \tag{10}$$

where $\theta(h)$ is the soil water content at matric potential h (mm), θ_s (mm) and θ_r (mm) are the residual and saturated soil water contents, α (1/mm) is the inverse air-entry suction parameter, $m = 1 - 1/n$ with n describing the pore size distribution.

The unsaturated hydraulic conductivity was calculated by

$$K(\theta) = K_s S_e^l \left[1 - \left(1 - S_e^{1/m}\right)^m\right]^2, \tag{11}$$

with

$$S_e = \frac{\theta - \theta_r}{\theta_s - \theta_r}, \tag{12}$$

where K_s (mm/h) is the saturated hydraulic conductivity, l is the pore-connectivity parameter (commonly set to 0.5). All the parameters in the van Genuchten equation were defined by model calibration in this study.

(2) Evapotranspiration

Table 2
Information and comparison of different soil moisture model configurations.

	SL	Revised model structure				Aqua Crop
		R-FLX	R-FLX-ET	R-FLX-ET-DRN	R-FLX-ET-INF	
Soil moisture redistribution	Not considered	Gradient of soil matric potentials (Buckingham-Darcy equation); both downward and upward soil water flux are considered				Tipping bucket method
ET_0	Penman Monteith	Penman Monteith	Penman Monteith	Penman Monteith	Penman Monteith	Penman Monteith
ETp	ET_0×Crop coefficient	ET_0×Crop coefficient	ET_0×Crop coefficient	ET_0×Crop coefficient	ET_0×Crop coefficient	ET_0×Crop coefficient
Actual soil evaporation	Not considered	Not considered	Consider soil moisture stress	Consider soil moisture stress	Consider soil moisture stress	Consider soil moisture stress and canopy cover
Root water uptake	Not considered	Not considered	Consider soil moisture stress and empirical coefficients	Consider soil moisture stress and empirical coefficients	Consider soil moisture stress and empirical coefficients	Consider root density and soil moisture stress
Actual crop transpiration	Not considered	Not considered	Sum of root water uptake of each layer	Sum of root water uptake of each layer	Sum of root water uptake of each layer	Sum of root water uptake of each layer
Drainage	Based on soil field capacity	Based on soil field capacity	Based on soil field capacity	Buckingham-Darcy equation	Based on soil field capacity	Based on soil field capacity
Infiltration	Fixed limitation	Fixed limitation	Fixed limitation	Fixed limitation	Horton equation	Fixed limitation
Vertical soil discretization	Single layer	Any number	Any number	Any number	Any number	Any number
Timestep	Sub-daily	Sub-daily	Sub-daily	Sub-daily	Sub-daily	Daily only

Evapotranspiration from the different soil layers has been considered, with evaporation and transpiration from the first layer while only transpiration from the deeper layer(s). Different evapotranspiration coefficients were therefore used to represent the varying evapotranspiration contributions. Specifically, *Ke* was introduced to represent evaporation for the first layer, and different crop efficiency K_b were introduced to represent the transpiration for different layers respectively. For transpiration, a water stressed index *Ks* was also calculated for each layer to adjust the reference evapotranspiration The revised evapotranspiration was accordingly calculated by

$$ET = ETe + ETc = ET_0 \times Ke + ET_0 \times Ks \times K_b, \tag{13}$$

where the water-stress factor *Ks* is given by Allen et al. (1996) as

$$Ks = \begin{cases} 0 & \theta \le \theta_{WP} \\ \dfrac{\theta - \theta_{WP}}{\theta_{FC} - \theta_{WP}} & \theta_{WP} < \theta < \theta_{FC} \\ 1 & \theta \ge \theta_{FC} \end{cases}, \tag{14}$$

in which θ represents the soil moisture content, θ_{FC} is the field capacity, θ_{WP} is the wilting point, and K_b represents a calibrated crop coefficient.

(3) Drainage

While the SL model defined drainage solely based on the field capacity threshold, the revised drainage component accounts for additional drainage driven by the soil water potential gradient between the root zone layer and the underlying layer, as described by the Buckingham–Darcy equation (Eq. (9)).

(4) Infiltration

The SL model uses two parameters (*Rain_minpen* and *Rain_maxpen*) to control the amount of rainfall infiltrating into the soil. However, infiltration capacity changes as a rain event progresses due to changes in the soil moisture content. Therefore, the Horton infiltration equation (Horton, 1933) was introduced to consider the infiltration according to

$$f(t) = f_c + (f_0 - f_c)e^{-kt}, \tag{15}$$

where $f(t)$ means infiltration rate at time *t*, f_c denotes steady state infiltration rate, f_0 is the initial infiltration rate, and *k* is a decay constant. In this study, f_c was set as the near-surface saturated hydraulic conductivity Ks_1, while f_0 and *k* were defined by model calibration.

2.3.3. Multi-layer framework

A multi-layer framework was developed to extend the optimized two-layer model structure. To investigate the influence of vertical discretization and parameterization on simulation accuracy, the soil profile was first divided into horizons with distinct hydraulic properties. Each horizon was then further discretized into multi-layers that shared the same parameter values.

2.3.4. Aqua crop model

Aqua Crop is a crop growth simulation model developed by the Food and Agriculture Organization of the United Nations (FAO) and has been widely used in agricultural water management across different crops (Raes et al., 2009; Steduto et al., 2009). Aqua Crop simulates soil water dynamics by dividing the soil profile into a series of compartments, each characterized by its hydraulic limits of saturation, field capacity, and wilting point. Rainfall and irrigation first infiltrate into the uppermost compartment, with an empirical exponential drainage function used to simulate the redistribution of soil moisture when it exceeds field capacity according to

$$\frac{\Delta\theta_{i,t}}{\Delta t} = \left(\theta_{i,t} - \theta_{fc,i}\right) \times f(\tau_i), \tag{16}$$

where $\theta_{i,t}$ is the soil moisture for *ith* layer at time *t*, and τ_i is a drainage time constant linked to soil hydraulic conductivity by $\tau_i = 0.0866K_s^{0.35}$. The soil moisture redistribution used is according to a bucket-type redistribution scheme. More detailed information about Aqua Crop can be found in Raes et al. (2009), with the difference between Aqua Crop and the soil moisture models developed in this study listed in Table 2. To ensure a fair comparison, the same layer thickness as in the two-layer model was applied in Aqua Crop, and all parameters were calibrated using the same objective function and optimization procedure, without relying on default parameter values for soil moisture estimtaions.

2.4. Model calibration and evaluation

Various global optimization approaches, such as Shuffled Complex Evolution (SCE-UA), Particle Swarm Optimization (PSO; Kennedy and Eberhart, 1995), and Genetic Algorithm (GA; Franchini, 1996), are widely used for calibrating soil moisture models, with SCE-UA adopted in this study due to its demonstrated robustness in handling multi-parameter problems and its widespread application (Duan et al., 1993; Khakbaz et al., 2012; Tang et al., 2024). The original SCE-UA algorithm is based on the simplex method, using multiple simplexes to search the solution space while updating points dynamically through a shuffling algorithm. Moreover, it uses a multi-start search approach, beginning with a set of initial solutions. These solutions are grouped into "complexes", with each complex generating new candidates using the simplex method. The shuffled and restructured population continues evolving to improve optimization. The Competitive Complex Evolution (CEE) algorithm was later developed to help generate candidate solutions within SCE-UA, which was also applied in this study (Vrugt et al., 2003; Wu et al., 2025).

Several statistical indices were selected to calibrate model parameters and evaluate simulation performance, including Nash-Sutcliffe Efficiency (NSE), Correlation Coefficient (R), Root Mean Square Error (RMSE) and Bias. Their calculations are based on

$$NSE = 1 - \left[\sum_{i=1}^{n} \left(\theta_{obs,i} - \theta_{sim,i}\right)^2 \Big/ \sum_{i=1}^{n} \left(\theta_{obs,i} - \overline{\theta}_{obs}\right) \right], \tag{17}$$

$$R = \frac{\sum_{i=1}^{n} \left(\theta_{obs,i} - \overline{\theta}_{obs}\right)\left(\theta_{sim,i} - \overline{\theta}_{sim}\right)}{\sqrt{\sum_{i=1}^{n} \left(\theta_{obs,i} - \overline{\theta}_{obs}\right)^2 \sum_{i=1}^{n} \left(\theta_{sim,i} - \overline{\theta}_{sim}\right)^2}}, \tag{18}$$

$$RMSE = \sqrt{\frac{1}{n} \sum_{i=1}^{n} \left(\theta_{obs,i} - \theta_{sim,i}\right)^2}, \tag{19}$$

$$Bias = \frac{1}{n} \sum_{i=1}^{n} \left(\theta_{sim,i} - \theta_{obs,i}\right), \tag{20}$$

where θ_{obs} represents the soil moisture measurements, θ_{sim} is the model-simulated soil moisture, and the overbar means the average value for each variable. NSE and RMSE, representing the dynamics and errors of the simulated soil moisture, were used as objective functions during model calibration. In the calibration process, NSE and RMSE were computed for all layers, with equal weighting assigned to each layer to ensure a balanced assessment of model performance throughout the soil profile.

2.5. Parameter sensitivity analysis

Model parameters substantially influence simulation accuracy, though their sensitivity varies. Calibrating all parameters may enhance performance but can also increase uncertainty and reduce computational efficiency, especially as the model complexity increases, i.e. in the case of multi-layer models. To identify the most influential parameters, a sensitivity analysis was conducted using the optimized two-layer model, and parameters identified as sensitive allowed to vary across horizons for the multi-layer soil moisture model (Fig. 3).

The Morris method (Morris, 1991) was applied to simplify the selection process for the multi-layer configuration. This is a screening method for identifying a subset of inputs that are influential on outputs, including those involved in interactions, based on elementary effects using a "one-factor-at-a-time" design of experiments (Demaria et al., 2007; Scollo et al., 2008). The elementary effect of each parameter is defined as

$$d_j = \frac{f(x_1, \ldots, x_j + \Delta, \ldots, x_n) - f(x_1, \ldots, x_j, \ldots, x_n)}{\Delta}, \quad (21)$$

where $f(X)$ is the objective function of the model, $X = (x_1, x_2, \ldots, x_n)$ is the n-dimensional vector of parameters, Δ denotes one step ($\Delta = \frac{p}{2(p-1)}$) between $1/(p-1)$ and $1 - 1/(p-1)$, and p is the number of levels into which the parameter space is discretized. In this study, p was set as 8 to balance the resolution and efficiency (Campolongo et al., 2007; Saltelli et al., 2010). Values of X were selected from the hyperspace Ω, identified by an n-dimensional p-level grid.

The mean (μ, assessing the overall influence of the parameter on the model accuracy) and standard deviation (σ, estimating non-linearity or interactions with other parameters) for each parameter were then calculated to quantify the parameter sensitivity based on

$$\mu_j = \sum_{i=1}^{n} |d_j(i)| \Big/ n \quad (22)$$

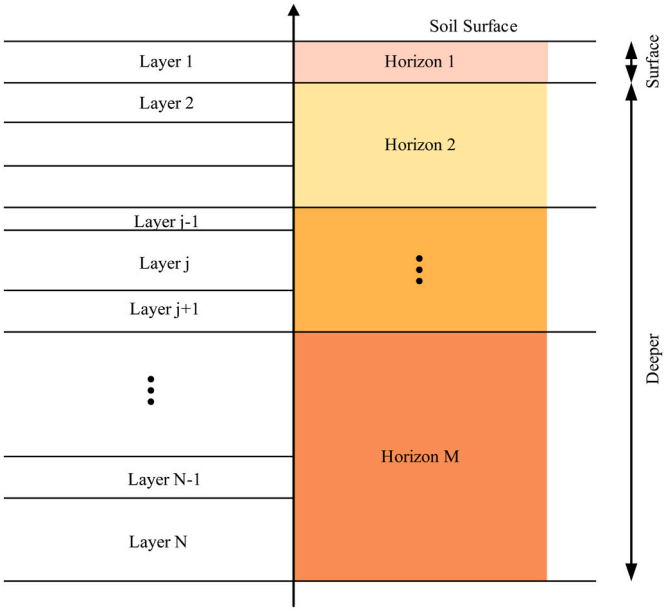

Fig. 3. Framework of the multi-layer soil moisture model. The surface layer was fixed at 5 cm to align with UAV-based observations, while the deeper soil profile was divided into multiple horizons with distinct parameters; layers within each horizon shared the same parameter values.

$$\sigma_j = \sqrt{\sum_{i=1}^{n} \left(d_j(i) - \frac{\sum_{i=1}^{n} d_j(i)}{r} \right)^2 \Big/ n}, \quad (23)$$

where μ^* is the absolute average value of μ and parameters with high μ^* indicate the overall importance of the parameter on model accuracy, while a large measurement of σ suggests that the parameter exhibits a non-linear behavior on the model accuracy or involves interaction with other parameters. The most influential parameters are those located in the top-right of a σ versus μ^* plot, where both sensitivity measures are high (Ben Touhami et al., 2013; Campolongo et al., 2007).

3. Results and discussion

3.1. Two-layer model simulations

3.1.1. Impact of model components

To systematically evaluate the influence of the model components (i.e., soil moisture redistribution flux, evapotranspiration scheme, deep drainage and infiltration) on simulation performance, a two-stage comparison framework was adopted. In the first stage, model structure assessments were conducted utilizing data from Station 6, selected for its data completeness and quality. The primary objective of this stage was to identify key components that substantially improved model performance, stability, or physical consistency. In the second stage, the selected model configuration was then applied to the remaining stations to assess predictive capability and generalizability, and to understand the impact of any site-specific variability. Two-layer model simulations were conducted using both daily and hourly forcing datasets to support component selection. To provide a baseline for evaluating the efficiency of the two- and multi-layer models, results from the SL model were also computed over the same time period. For the SL model, soil moisture measurements from all nine depths were weighted based on the soil thickness to represent the reference ("truth") soil moisture. For the two- and multi-layer models, soil moisture observations from the 0–5 cm sensor were used as the reference for the near-surface layer to align with UAV-based radiometer retrievals, while the weighted average of the remaining corresponding depths was used to represent the reference values for deeper layers. All the parameters calibrated in the two-layer models were detailed in Table S6.

Results based on the SL model are shown in Fig. 4, with relatively good results for daily-based simulations but a poor performance for hourly simulations. The reason for this is that a one-layer bucket model is capable of representing the soil moisture dynamics corresponding to rainfall/irrigation events for a coarse temporal resolution, while it is unable to correctly capture the dynamics at finer temporal resolution.

Overall simulation performance based on a two-layer model with alternative component representation is presented in Fig. 5. Statistics, including NSE, R, RMSE and bias are listed in Tables S1 and S2 and the values of calibrated parameters are listed in Table S7. The Taylor diagrams in Fig. 5 illustrate the relative performance of different model configurations in terms of correlation, standard deviation, and centered root mean square error, for both near-surface and root zone soil moisture under daily and hourly forcing. When comparing the simulation results across model configurations and their conceptualizations, each additional process incorporated into the model influenced simulation performance in a distinct way. Detailed comparisons of these differences are as follows.

The two-layer baseline model, which simulates vertical soil moisture redistribution using the Buckingham-Darcy equation (R-FLX), captured the general dynamics of both the near-surface and RZSM under rainfall and irrigation events, with R = 0.8788 and RMSE = 0.0369 cm^3/cm^3 for the near-surface, and R = 0.9343 and RMSE = 0.0273 cm^3/cm^3 for root zone (Table S1). Hourly simulations (Table S2) improved temporal

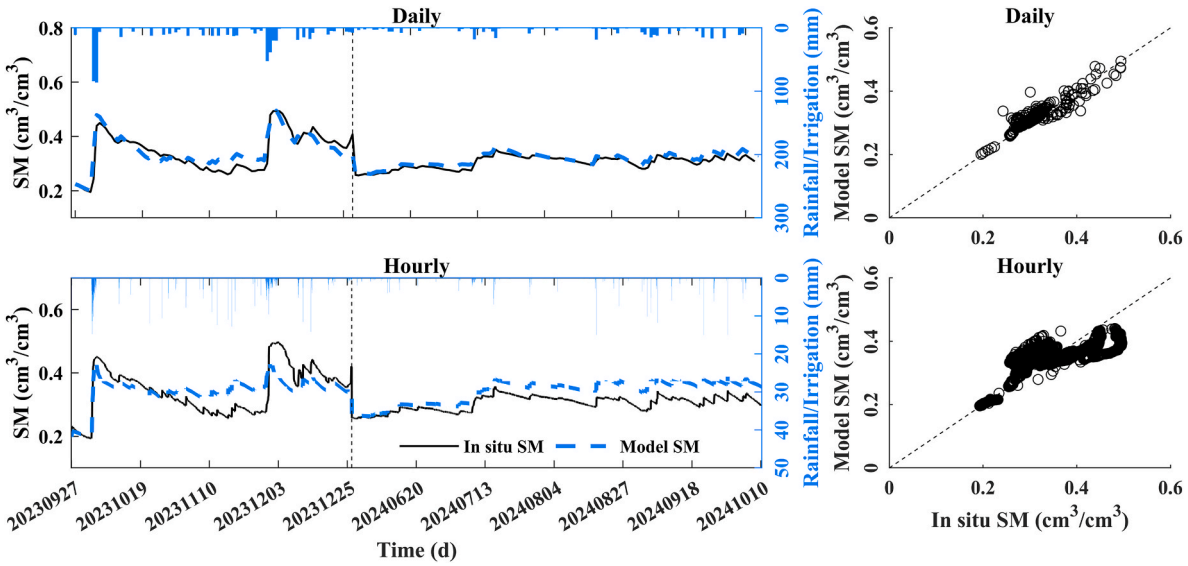

Fig. 4. Soil moisture simulation results based on the single-layer (SL) model at Station 6 using hourly and daily forcing data.

responsiveness, particularly in the near-surface layer (NSE = 0.8344, R = 0.9139), demonstrating the value of finer temporal resolution. Accordingly, when using hourly rainfall data, the near-surface layer displayed greater fluctuations due to the rapid response to the precipitation, while the root zone showed similar smooth changes. This difference arises because rainfall and irrigation typically occur as short intense events, while infiltration and redistribution processes operate over longer timescales. Compared to the SL model, the two-layer R-FLX model provided more realistic dynamics when applied with hourly rainfall data, increasing the NSE of soil moisture estimations by up to 75% in calibration, and turning the negative NSE in the validation period to positive, highlighting the limitation of bucket-type models. By explicitly representing soil moisture fluxes between layers, the R-FLX model captured moisture gradients and water exchange driven by soil moisture conditions, thereby improving the representation of natural redistribution processes in layered soils and yielding a more reliable simulation. As the interaction between soil layers is critical important when utilizing near-surface information to enhance the accuracy of RZSM simulation, soil moisture redistribution based on the Buckingham-Darcy equation was kept for latter applications.

Evapotranspiration algorithm was further revised based on the two-layer model R-FLX (named R-FLX-ET, Table 2) with the simulation results for both the near-surface layer and root zone layer shown in Figs. S3–S4. Under daily meteorological forcing, the NSE of RZSM estimations improved from 0.8535 (R-FLX) to 0.9054, while bias decreased from 0.0092 cm^3/cm^3 to 0.0024 cm^3/cm^3. A similar trend was observed in simulations based on hourly meteorological forcing, where the RZSM NSE improved to 0.9152 and R improved to 0.9600. These results indicate that the revised evapotranspiration scheme enhanced deep-layer soil moisture prediction accuracy, although at the cost of minor near-surface degradation. During the validation period at Station 6, the R-FLX-ET model effectively captured the temporal dynamics of near-surface soil moisture, accurately reproducing the timing and general trends of wetting and drying cycles (Figs. S3–S4), which was also reflected by a correlation of 0.8060 and an RMSE of 0.0473 cm^3/cm^3. The moderate positive bias of 0.0379 cm^3/cm^3 indicated a slight overestimation of surface moisture, particularly following wetting events. Despite this overestimation in magnitude, the model maintained a consistent ability to track the observed near-surface moisture fluctuations. For the root zone, the model exhibited even stronger performance, with an excellent correlation of 0.9661, very low RMSE of 0.0116 cm^3/cm^3, and near-zero bias of −0.0096 cm^3/cm^3, demonstrating the model's ability to accurately simulate the smoother and slower dynamics of deeper soil moisture during the validation period, further confirming its reliability and stability. For the near-surface layer, the temporal change of soil moisture fluctuated less while the soil moisture in the root zone reduced due to the higher transpiration rate (Figs. S3–S4). Accordingly, evapotranspiration calculation considering the coupling with soil moisture as implemented here led to a better estimation of soil moisture for the different soil layers.

Compared with R-FLX, the NSE of RZSM based on R-FLX-ET increased by 6% and 10% for the calibration and validation periods, separately. The importance of incorporating the coupling relationship between soil moisture and evapotranspiration has been proven in past studies (Dong et al., 2020; Zhao et al., 2025). Moreover, accounting for layer-specific crop coefficients (K_b) is important, as both the K_b values and root depth definitions vary among crop types (Allen et al., 1996; Pereira et al., 2015a). Consequently, revising the evapotranspiration component was essential for ensuring applicability across different cropping seasons. Given that detailed K_b values have been well established for various crops (Allen et al. 1996, 2006), they can be effectively used to improve soil moisture estimation. Based on these considerations, further model development here was conducted using the R-FLX-ET framework.

Subsequent modification of the drainage component in R-FLX-ET called R-FLX-ET-DRN, led to a decreased simulation accuracy, particularly for the near-surface soil moisture estimations and using daily forcing data (Figs. S5–S6). The NSE of near-surface soil moisture simulations dropped to 0.6903 using daily inputs and to 0.7072 using hourly inputs. For RZSM, the NSE based on daily meteorological forcing dropped to 0.7354, while the NSE decline was less pronounced when using hourly meteorological forcing data (0.9115), but still less favorable than for the preceding model. Consequently, the original drainage formulation was retained to preserve structural simplicity.

The drainage calculation has been considered as a bottom boundary condition in literature (Campoy et al., 2013; Chen et al., 2018; He et al., 2021; Zeng and Decker, 2009). Accordingly, in this study the original model with drainage calculated based on field capacity can be regarded as a free drainage boundary, while calculation based on the Buckingham-Darcy equation can be regarded as a moisture limited boundary condition that is impacted by the moisture content of the adjacent soil layer. The influence of drainage on soil moisture estimation can be varied. Specifically, Chen et al. (2018) demonstrated that the impact of drainage on soil moisture estimation generally increased with soil depth and decreased with time. While Zeng and Decker (2009) indicated a substantial effect of the drainage calculation on soil moisture

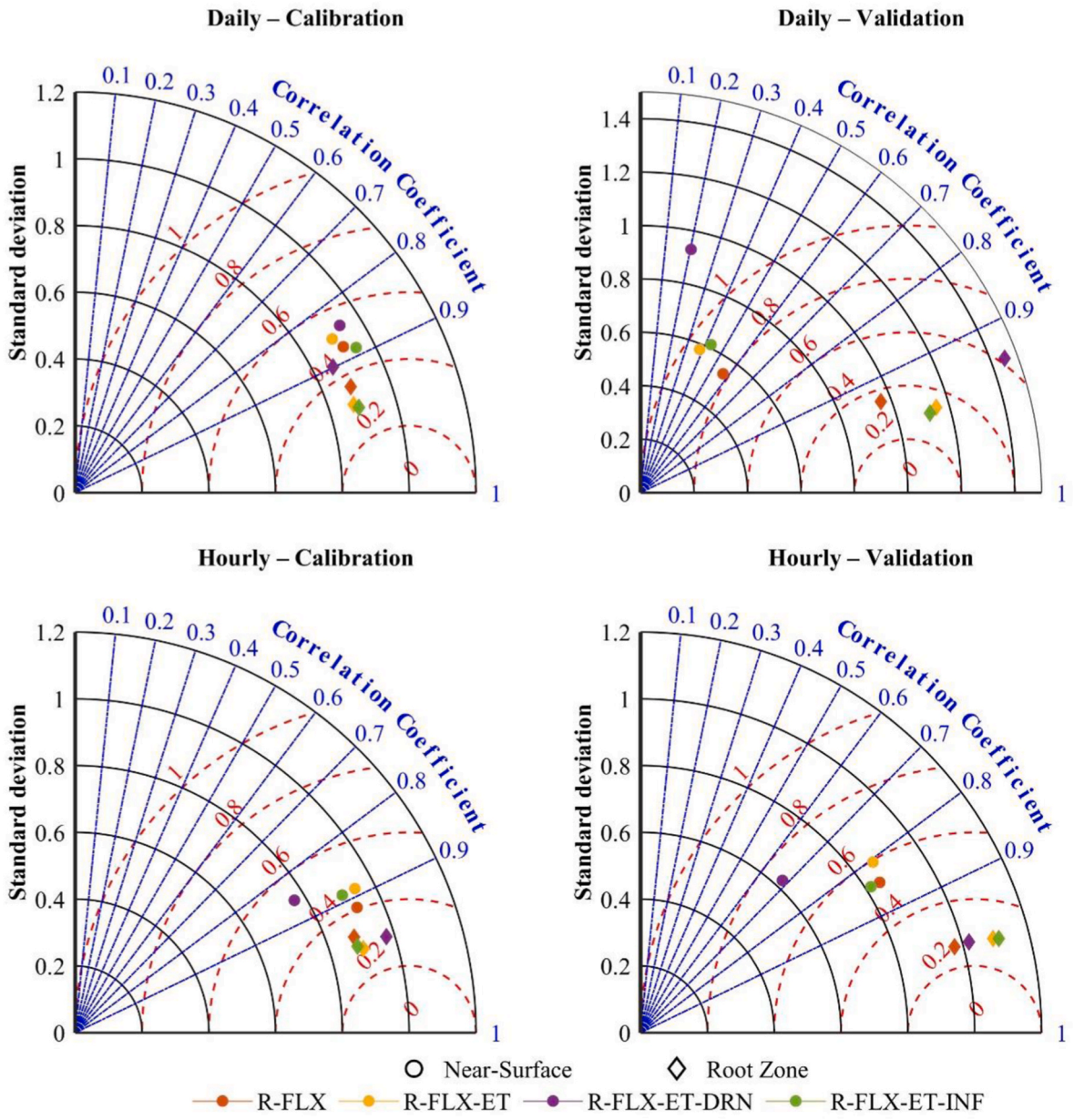

Fig. 5. Taylor diagram of simulation results from two-layer models with different component configurations (Table 2) using daily (left) and hourly (right) meteorological data. Circle markers represent the near-surface layer, and diamond markers represent the root zone soil moisture (RZSM).

estimation, the results of He et al. (2021) showed only a subtle impact, especially for a Sand Loam soil overlaying a Clay Loam, being the condition for our study area. Moreover, the relationship between drainage calculation and soil texture was also explored by Campoy et al. (2013), with only minor improvements on the accuracy of soil moisture simulation, which was consistent with the findings in this study.

Introducing a revised infiltration in R-FLX-ET using the Horton equation, called R-FLX-ET-INF, resulted in a subtle improvement to RZSM estimates using both daily (NSE = 0.9167; RMSE = 0.0206 cm^3/cm^3) and hourly (NSE = 0.9073; RMSE = 0.0220 cm^3/cm^3) meteorological forcing. The performance of R-FLX-ET-INF over R-FLX-ET was more pronounced for near-surface soil moisture estimations, especially when using daily meteorological forcing (NSE = 0.7297 for R-FLX-ET versus 0.7846 for R-FLX-ET-INF) than for using hourly meteorological forcing (NSE = 0.7874 for R-FLX-ET versus 0.7903 for R-FLX-ET-INF). According to the temporal dynamics (Figs. S7–S8), near-surface moisture estimation was more sensitive to rainfall events under hourly forcing (Table S2), demonstrating that the additional infiltration component helped the soil moisture model to more accurately mirror the fluctuations in soil moisture response to rainfall and irrigation events. The importance of infiltration on soil moisture estimation has been previously demonstrated from different aspects, including calculation methods (Feki et al., 2018; Zhang et al., 2024) and infiltration pathways (Meng et al., 2023), which align with the results of this study. However, the influence of infiltration on the soil moisture estimation has also been found to present a decreased impact with increasing soil depth, especially when considering satellite-derived near-surface soil moisture information (Zhang et al., 2024). Compared with R-FLX-E, the RZSM accuracy based on R-FLX-ET-INF improved around 2% for NSE and around 5% for RMSE for both the calibration and validation periods. However, the improvement was insufficient to justify incorporating variable infiltration as an additional aspect to the soil moisture model, due to its complex representation and two extra parameters requiring calibration, which are difficult to define using standardized values. Therefore, the original formulation was retained to preserve the model's parsimony while maintaining satisfactory performance. Considering the

possible disturbance caused by livestock in the field, the influence of water ponding, presented by a calibrated maximum ponding storage, was also tested. The results (not shown) indicated that including this process did not lead to an improvement in model performance compared with the R-FLX-ET model. In particular, the near-surface soil moisture exhibited an overly sensitive response to rainfall events in the validation period, which can be attributed to the prolonged influence of surface water storage on infiltration dynamics. The performance of the two-layer R-FLX-ET model was further compared with Aqua Crop, one of the most widely used agricultural water management models (Pereira et al., 2015b; Pinheiro et al., 2024; Saab et al., 2015). Compared with R-FLX-ET, Aqua Crop calculates soil moisture redistribution based on drainage schemes without explicitly accounting for soil gradients, and estimates evapotranspiration by considering both soil moisture stress and canopy stress. Since Aqua Crop is designed for daily application, the comparison was conducted on a daily timestep (Fig. S3, Table S1). To ensure consistency, the soil profile in Aqua Crop was represented by two layers: 0–5 cm for the near-surface and 5–60 cm for the root zone, aligning with the structure of R-FLX-ET. Importantly, R-FLX-ET reproduced both the timing and magnitude of surface soil moisture variations more accurately than Aqua Crop, especially for the root zone layer during the validation period (Fig. S3). Soil moisture peaks after rainfall and irrigation events were better captured in R-FLX-ET, whereas Aqua Crop tended to underestimate the wetting response and dampen short-term fluctuations. This difference was also reflected in the performance statistics. R-FLX-ET showed improved performance thanAqua Crop in simulating RZSM for both the calibration and validation period, achieving higher NSE (0.9054 vs. 0.7836 for calibration and 0.8792 vs. −2.9673 for validation), indicating a closer agreement with observed variability and greater temporal consistency across time periods. Aqua Crop, with its bucket-type water balance, tended to dampen fluctuations and underestimate soil moisture under wet conditions, whereas R-FLX-ET more effectively represented vertical water redistribution, demonstrating the importance of using the Buckingham-Darcy equation to calculate the soil moisture redistribution (van Dam and Feddes, 2000; Vereecken et al., 2016). The debate of using physically-based principles (flow controlled by gradients such as soil moisture redistribution based on the Buckingham-Darcy equation) versus applying a more simplistic model with cascade flow has been widely discussed, with the former method found to outperform the latter (MacBean et al., 2020; Tsiros et al., 1998; Vianna et al., 2024). The results of this study further emphasize the importance of considering the soil moisture gradient when representing soil moisture redistribution. In terms of evapotranspiration, revision based on soil moisture stress might be sufficient for providing good soil moisture estimations, compared to Aqua Crop that considers both soil moisture and canopy stress.

Among the tested revisions, soil moisture redistribution based on the Buckingham–Darcy equation and the revised evapotranspiration formulation were found to have the greatest impact on model accuracy. While variable infiltration could also enhance the model accuracy slightly, the additional parameters and complexity outweighed the benefits. The R-FLX-ET model thus provided an effective balance between accuracy and parsimony, making it the preferred configuration for further development. Compared with both the SL and Aqua Crop models, R-FLX-ET could also provide more accurate soil moisture estimations driven by forcing data at different temporal resolutions.

All four two-layer models generally provided satisfactory performance (NSE $\geq$0.70 for the near-surface layer and NSE $\geq$0.85 for the RZSM driven by hourly forcing data. Those soil moisture models consistently yielded better performance by using hourly rainfall data, capturing the temporal dynamics of near-surface soil moisture more accurately, compared with using daily rainfall data. While daily simulations produced reasonable results, they failed to reflect the rapid surface fluctuations observed during rainfall and irrigation, likely due to their coarse temporal resolution. This is consistent with the finding of Filippucci et al. (2020), who addressed the importance of finer temporal resolution in soil moisture estimation during irrigation. Accurate representation of near-surface soil moisture has important implications for using UAV-based near-surface information to improve the accuracy of RZSM estimates. Therefore, hourly meteorological forcing is recommended for future application. In practice, hourly precipitation/irrigation information can be obtained from dense rain gauge networks, satellite-based products, or weather model outputs, and can also be readily measured at the farm scale using standard rain gauges. Hourly evaporation can be approximated by disaggregating daily estimates from widely used products such as GLEAM (Global Land Evaporation Amsterdam Model; Miralles et al., 2025).

3.1.2. Model numerical stability

Given the influence of time step size on simulation accuracy, numerical stability was evaluated. The numerical stability assessment was conducted using the two-layer R-FLX-ET model, identified as the balanced configuration in terms of performance and complexity. Three numerical schemes were implemented and compared: (1) the original model employing an explicit scheme with a fixed time step size, (2) an implicit form of the Buckingham-Darcy equation with a fixed time step size, and (3) a variable time step size approach, in which time step size reduced until the difference between the two-half-step estimates and full-step estimate fell below a predefined threshold (set as 0.1% of layer depth in this study). The stability and performance of the three numerical schemes were evaluated under both daily and hourly temporal resolutions (Fig. 6), enabling a comprehensive comparison of their robustness across different time scales.

All three numerical schemes produced consistent soil moisture simulations that closely matched in-situ observations, confirming the model's strong numerical stability across temporal resolutions and formulations. The time series (left panels) and scatter plots (right panels) in Fig. 6 show that all methods reproduced the temporal dynamics of soil moisture with minimal divergence and a high agreement with observations. Across methods, NSE values generally exceeded 0.70 for the near-surface and 0.89 for the root zone, with corresponding correlation coefficients above 0.84 and 0.91, RMSE below 0.040 $cm^3\ cm^{-3}$, and biases near zero. RZSM estimations based on the three numerical schemes presented a higher consistency than for the near-surface layer, likely due to the damping effect of deeper soil layers, which reduces sensitivity to short-term atmospheric forcing and numerical fluctuations. Despite minor differences, the close agreement among the three schemes demonstrated that the model structure is numerically stable and reliable under different computational settings. Additional to the relatively homogeneous soil profile in the study area, numerical stability of the R-FLX-ET model was also evaluated using data from the Los Coscolls station from the ISMN, characterized by a more heterogeneous soil profile (sandy loam over clay loam). The Buckingham-Darcy equation is one of the fundamental and commonly used equations to describe moisture redistribution between soil layers. Numerous methods have been proposed to achieve the desired accuracy and avoid unrealistic results (Ducoudre et al., 1993; He et al., 2021; Qi et al., 2018), with the numerical difficulties of using these equations having been carefully examined (Zha et al., 2017). However, it was found here that this equation can be solved explicitly to provide a good estimation. While the implicit and variable time step methods provided slightly smoother simulations and marginal improvements in RMSE for the near-surface layer, the overall differences in performance were minor. Given the increased computational complexity and cost associated with solving the implicit form and managing adaptive time stepping, these methods offered limited practical advantage in this context. Consequently, the approach of using an explicit form of the Buckingham-Darcy equation with a fixed time step was retained for all subsequent analyses in this study. The demonstrated stability and satisfactory accuracy of the R-FLX-ET model made it a suitable and practical choice for further application.

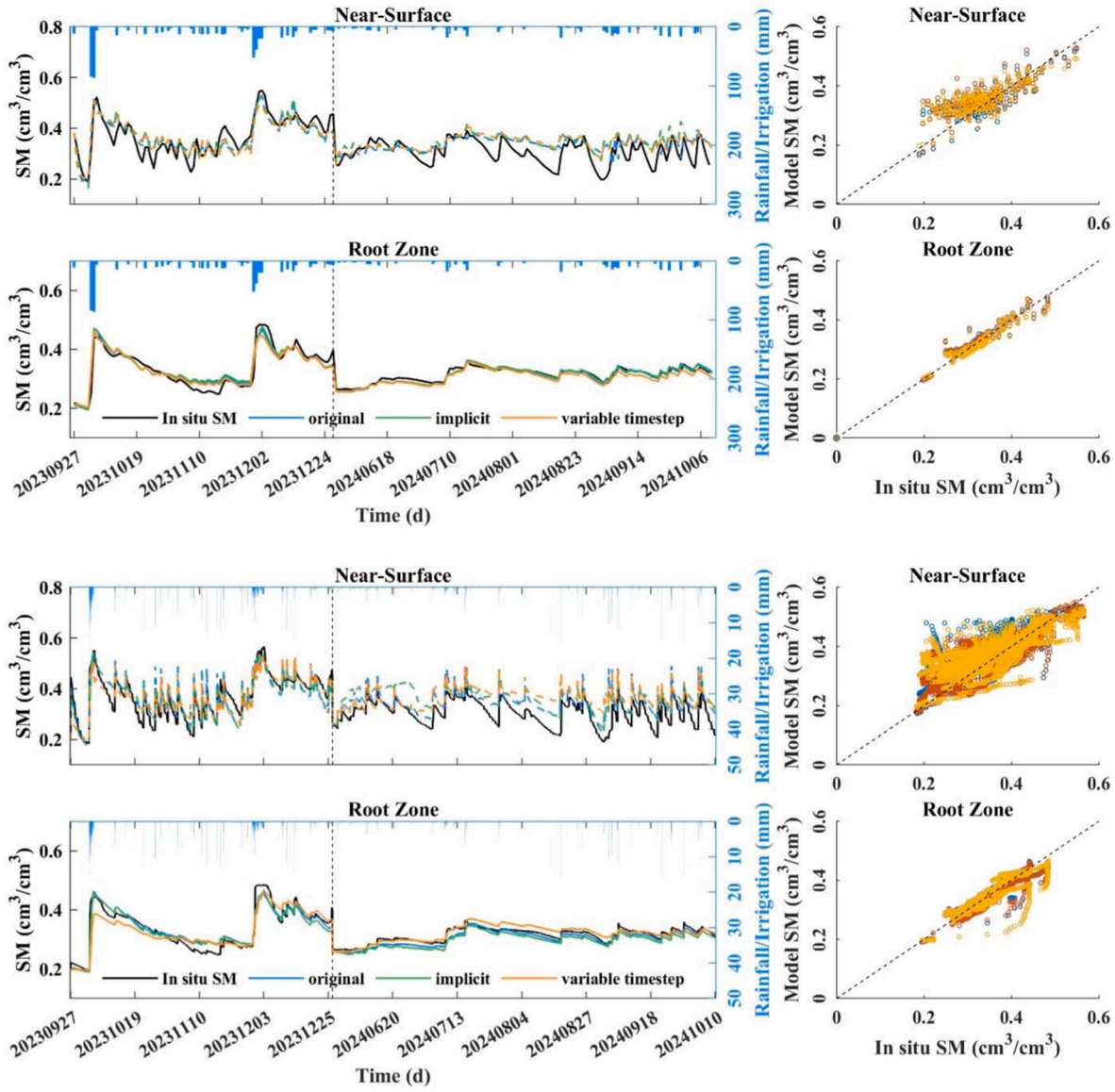

Fig. 6. Numerical stability of the model. Time series plots are shown in the left panels and scatter plots in the right panels, with results based on daily data at the top and hourly data at the bottom.

3.1.3. *Model evaluation across different stations*

The reliability of the two-layer R-FLX-ET model was evaluated at additional locations with available observations (Stations 2, 4, and 5; Fig. 7, Fig. S9–S10, Table S3) to assess its spatial robustness and generalizability. Station 2, where only rainfall serves as the hydrological input, provided a slightly different scenario to Station 6, which involved both rainfall and irrigation. R-FLX-ET achieved high correlation in both the calibration period (0.8623 for the near-surface and 0.9591 for the root zone), with low RMSEs (0.0300 and 0.0128 cm^3/cm^3, respectively), as well as in the validation period (R = 0.8550, RMSE = 0.0395 cm^3/cm^3 for the near-surface, R = 0.9465, RMSE = 0.0109 cm^3/cm^3 for the root zone). Importantly, the soil moisture model could capture rainfall-driven variations with high reliability, having only minor overestimations in the near-surface layer during wet conditions (Fig. 7). Points representing simulated and observed soil moisture clustered tightly along the 1:1 line with minimal bias for both layers and periods, particularly in the root zone, affirming the robustness of the R-FLX-ET model under rainfall-only conditions. At Station 4, where frequent irrigation was applied in addition to rainfall, the model also effectively captured the near-surface soil moisture dynamics. While R-FLX-ET slightly underestimated peak moisture values during intensive irrigation events, overall agreement with observations was strong. For the root zone, simulation accuracy was high, with R = 0.9631 and RMSE = 0.0189 cm^3/cm^3 during calibration, while R = 0.9429 and RMSE = 0.0052 cm^3/cm^3 during validation. Scatter plots showed excellent agreement in the root zone, though greater dispersion was noted for the near-surface layer, likely due to the irregularity of irrigation timing and intensity. At Station 5, the R-FLX-ET model reproduced near-surface moisture fluctuations reasonably well but tended to slightly overestimate moisture following irrigation events, especially during the validation period. For the root zone, slight underestimations were observed. Nonetheless, the soil moisture model maintained a coherent representation of soil moisture dynamics, demonstrating its applicability across varying stations.

At Station 2 (rainfed site), the R-FLX-ET model achieved high accuracy, as soil moisture dynamics were primarily driven by precipitation and evapotranspiration, which exhibit smoother temporal variability than the intensive inputs characteristic of irrigated sites (Evett et al., 2006; Techen et al., 2020; Vereecken et al., 2016). In contrast, irrigated sites exhibit additional short-term variability due to irrigation

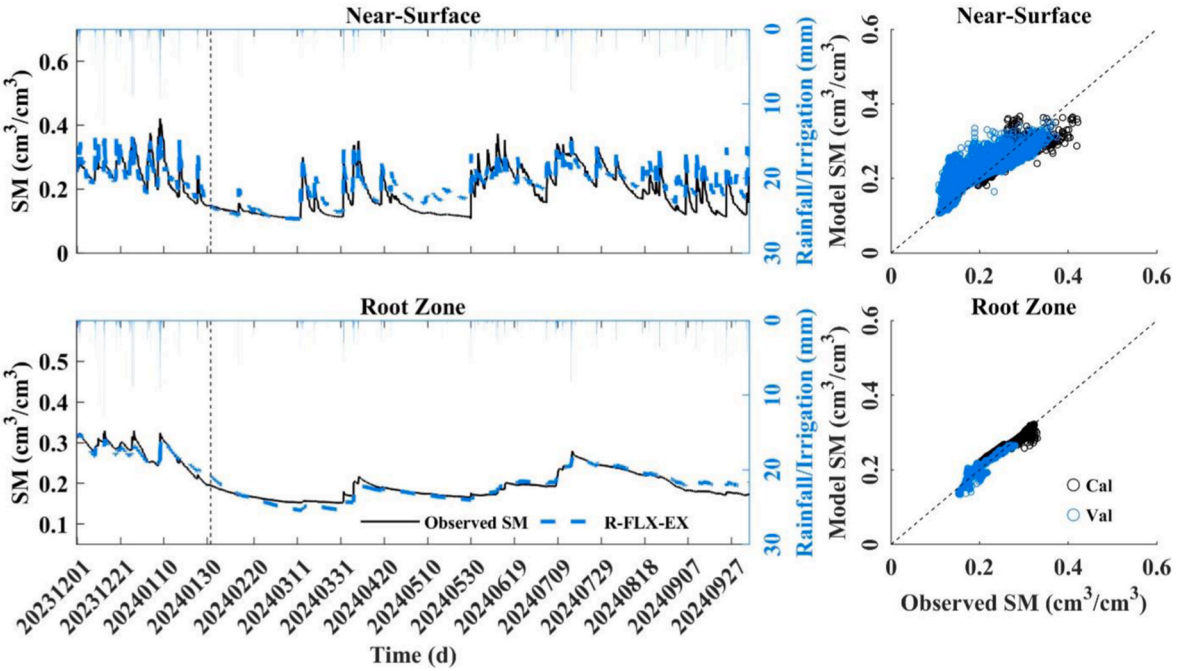

Fig. 7. Soil moisture estimation based on the two-layer model R-FLX-ET for Station 2 using an hourly forcing dataset. The time series to the left of the black line represents the calibration period, and that to the right represents the validation period.

applications, which can create spatial heterogeneity and sharper infiltration pulses. Nevertheless, the R-FLX-ET model was developed and calibrated using both rainfall and irrigation inputs, with the validation across irrigated sites demonstrating that it can effectively reproduce soil moisture under irrigation management as well. The soil moisture model demonstrated strong spatial and temporal reliability across the four stations under both rainfall-only and combined rainfall–irrigation conditions. Although surface simulations exhibited increased sensitivity to the complexity of irrigation, resulting in occasional over- or underestimation, the model consistently reproduced the soil moisture dynamics with high temporal correlation and acceptable error metrics. In contrast, the simulation of RZSM by the two-layer R-FLX-ET model remained stable across all stations, thereby confirming its robustness for field-scale applications. To further assess the performance of the R-FLX-ET model across different climate conditions, soil types, and crop seasons, daily and hourly datasets from four ISMN stations (Vallecitos, GrouseCreek, KyleCanyon, LosCoscolls) with diverse conditions, as well as one oat season from the study field were also used for model evaluation (results not shown). The results generally indicated consistent model performance across all conditions.

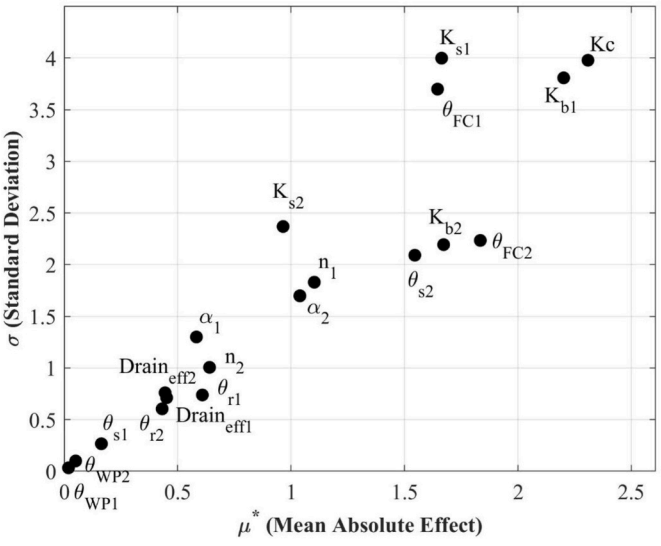

Fig. 8. Parameters sensitivity analysis based on the Morris method.

3.2. Multi-layer model simulation

3.2.1. Parameter sensitivity analysis

Based on the conclusions from the two-layer model analysis, a set of multi-layer models (R-FLX-ET_MUL) was developed. To improve model calibration efficiency and minimize model uncertainty, a parameter sensitivity analysis using the Morris method was conducted on the two-layer R-FLX-ET model. This analysis identified the most influential parameters in both the near-surface and root-zone layers, which were then selected for calibration for each layer in the multi-layer configurations tested. The scatter plot of μ* versus σ (Fig. 8) provided a visualization of both the magnitude and variability of each parameter's influence on model output. The sensitivity analysis results indicated that the evaporation factor K_c, crop efficiency (K_{b1}, K_{b2}), saturated hydraulic conductivity (K_{s1}, K_{s2}), field capacity (θ_{FC1}, θ_{FC2}), saturation percentage and inverse air-entry suction parameter for bottom layer (θ_{s2}, α_2) and pore size distribution for near-surface layer (n_1) are the most influential parameters, as evidenced by their high μ* versus σ values (Fig. 8). These parameters play a critical role in regulating water balance, evapotranspiration processes, and vertical water movement. In contrast, parameters including the wilting points (θ_{WP1}, θ_{WP2}), drainage efficiency ($Drain_{eff1}$, $Drain_{eff2}$), and residual moisture content (θ_{r1}, θ_{r2}) showed low sensitivity, suggesting limited influence on model output under the conditions evaluated. The sensitivity analysis results are consistent with previous studies, whereby soil moisture dynamics are controlled primarily by hydraulic parameters defining the shape of the soil water retention curve, while parameters defining lower-bound moisture conditions tended to exhibit comparatively lower sensitivity to model outputs (Bandara et al., 2013; Wöhling et al., 2008).

Based on these findings and considering the underlying physical mechanisms governing vertical water fluxes in multi-layer soil systems, a subset of key parameters was selected for layer-specific calibration in

the multi-layer model. These included saturated hydraulic conductivity (Ks), crop efficiency (K_b), saturation point (θs), field capacity (θ_{FC}), and inverse air-entry suction parameter (α) for each root zone layer, while other parameters were set as the same value for all the layers based on calibration. Ks was prioritized due to its direct control over the maximum flux between adjacent layers, which is essential for simulating vertical moisture redistribution. Moreover, K_b was retained to account for variation in layer-specific transpiration behaviour, being particularly relevant in deep-rooted systems. Finally, θ_s and θ_{FC} were included to represent the variability in soil water holding capacity and retention characteristics across layers, which are crucial for accurately modelling temporal changes in root zone moisture storage.

3.2.2. Impact of model horizons

Two sets of layer configuration scenarios were considered for the multi-layer soil moisture model, aiming to balance physical realism, functional relevance, and computational efficiency. To facilitate referencing, model names encode the structure of the vertical discretization, with the suffix indicating the number of layers followed by their thickness. When all layers differ, each thickness is listed explicitly (e.g., R-FLX-ET_MUL_3_051540 refers to three layers of thickness 5, 15, and 40 cm). When consecutive layers share the same thickness, a multiplier is used to denote repetition (e.g., R-FLX-ET_MUL_5_0515_4 corresponds to a 5 cm near-surface layer and four subsequent layers of 15 cm each). The first scenario adopted a simplified scheme based on vegetation characteristics, specifically the rooting profile of pasture, which is the dominant land cover over the period for model development. In this configuration, the soil profile was divided into three layers: a 5 cm near-surface layer, a 15 cm top root zone layer representing the primary active root depth, and a 40 cm sub root zone layer (R-FLX-ET_MUL_3_051540). This structure focused on the plant–soil interactions governing evapotranspiration and water uptake, while keeping the model parsimonious with fewer layers and fewer parameters to calibrate. The second scenario was based on the measured soil texture profile and provided a more detailed vertical discretization of the soil column. It consisted of a 5 cm near-surface layer followed by four sub root zone layers with thicknesses of 10 cm, 15 cm, 15 cm, and 15 cm (R-FLX-ET_MUL_5_0515_4), respectively. This design captured variations in soil hydraulic properties with depth and enabled more physically representative modelling of soil water redistribution processes, especially across interfaces with contrasting texture and permeability. All of the layers for these two multi-layer models were first regarded as being different soil horizons with different parameters, with the necessity of dividing them into more layers subsequently assessed. The results based on these two scenarios are shown in Figs. 9 and 10, Tables S4–S5. All the calibrated parameters can be referred to Table S8.

For the three-layer model R-FLX-ET_MUL_3_051540, simulated soil moisture exhibited strong agreement with both the temporal precipitation patterns and in situ observations during the calibration period across all layers, with correlation coefficients exceeding 0.88 and RMSE values below 0.04 cm^3/cm^3. During the validation period, similarly high accuracy was observed in the root zone layers, while the near-surface layer showed more rapid fluctuations, a slightly lower correlation of 0.6435, and minor underestimations. Nevertheless, the model adequately captured the dynamic response of soil moisture to rainfall and irrigation events, capturing the timing of soil moisture peaks but with underestimation of -0.0059 cm^3/cm^3. The peaks in soil moisture gradually spread with depth, indicating the time taken for water to infiltrate downwards. The five-layer model, R-FLX-ET_MUL_5_0515_4, also demonstrated satisfactory performance, achieving R values greater

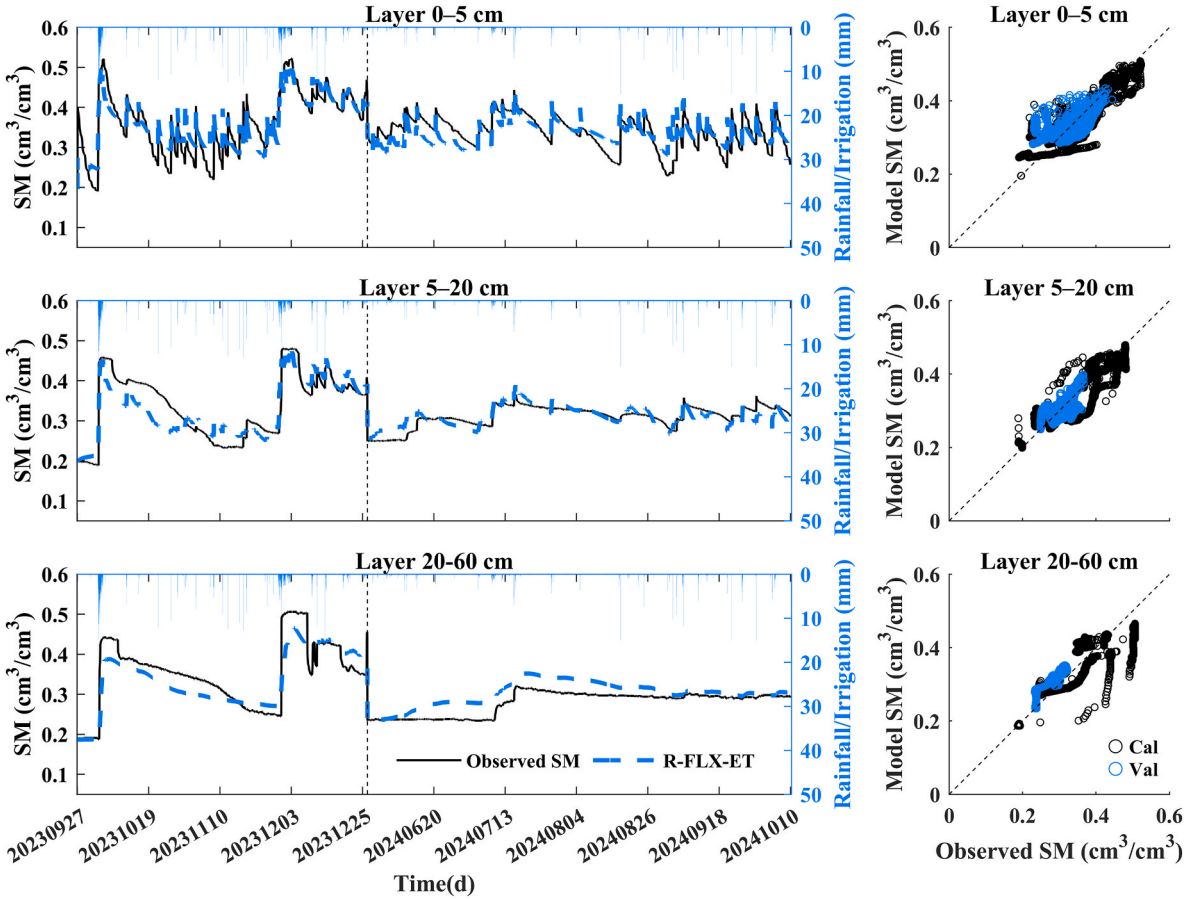

Fig. 9. Soil moisture estimation based on three-layer model R-FLX-ET_MUL_3_051540 with hourly forcing data. The time series to the left of the black line represents the calibration period, and that to the right represents the validation period.

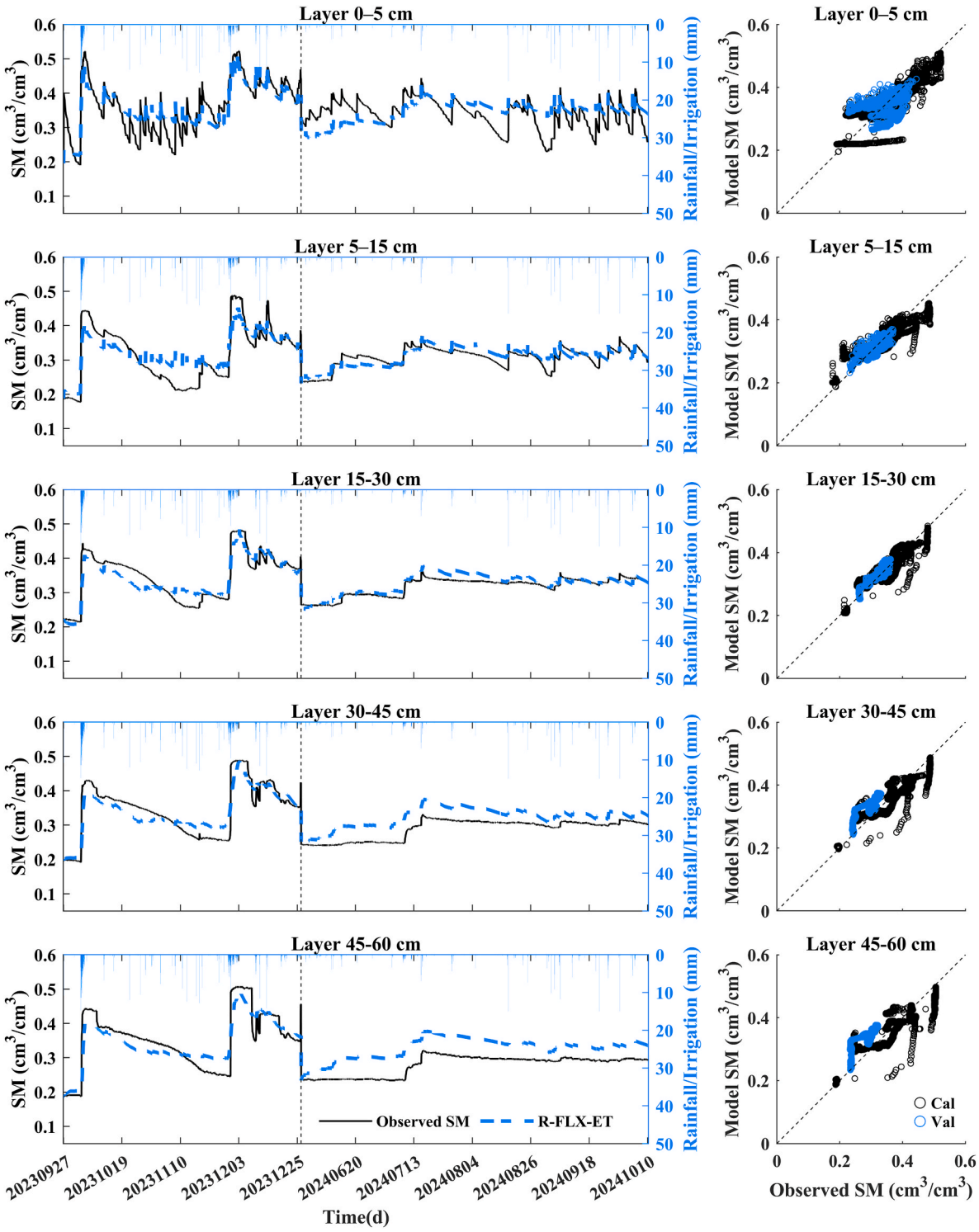

Fig. 10. Same as Fig, 9 but for R-FLX-ET_MUL_5_0515_4.

than 0.90 across all root zone layers during both the calibration and validation periods. However, the near-surface layer exhibited a reduced correlation with observed data during the validation period. For both multi-layer models, the center layer(s) presented the most balanced model accuracy, with a gradation in temporal dynamics that closely mirrored realistic soil behavior. Therefore, an increased number of soil layers provides more details about the profile soil moisture distribution.

To gain a better understanding of the influence of soil horizons, aggregated soil moisture values for the entire profile were compared based on model simulations with different layer configurations, as shown in Fig. 11. Time series soil moisture showed that the two-layer model responded most sharply to rainfall/irrigation events, while the five-layer model exhibited the smoothest dynamics and a tendency to underestimate soil moisture. In the scatter plot, the two-layer model showed greater spread around the 1:1 line, while the five-layer model clustered most tightly, especially for wet conditions. Despite these differences, all three models reproduced similar fluctuations and dynamics, and their overall performance was comparable, indicating that a finer

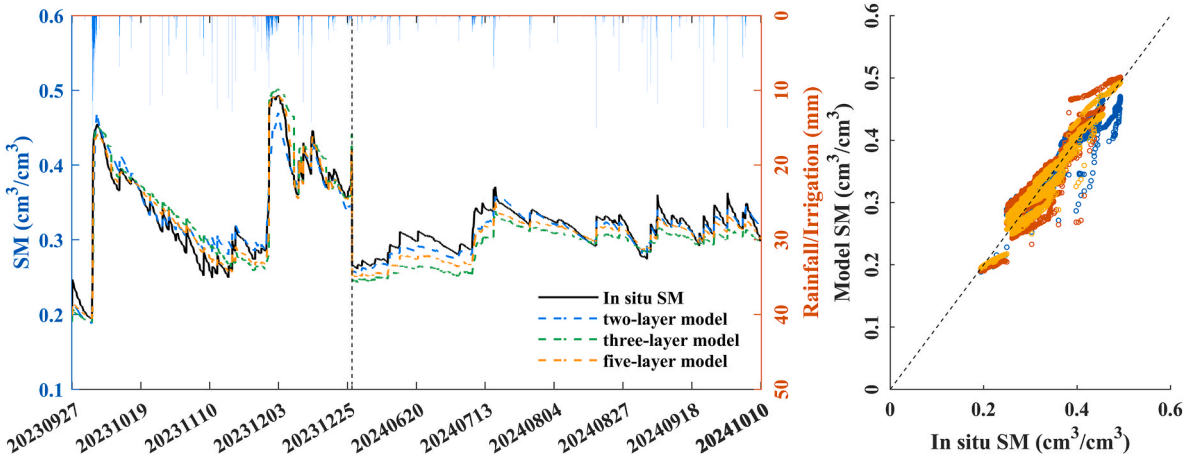

Fig. 11. Soil moisture simulations for the 0–60 cm soil profile using models with different horizon configurations.

vertical discretization did not bring substantial improvement to the model simulation results. This could be attributed to the relatively homogeneous soil conditions in the study area (loam-clay type), where limited vertical variability in hydraulic properties reduced the benefit of additional layer discretization. Moreover, the dominant processes controlling soil moisture dynamics were already effectively captured within the two-layer structure, and so further subdivision mainly refined internal gradients rather than introducing new governing processes. In addition, the increased number of layers introduces more parameters, and the calibration process may compensate for structural differences. This is consistent with findings in land surface modelling, where increased vertical resolution (e.g., moving from two-layer to 11-layer schemes) had a secondary impact compared to differences arising from parameterizations (Parrens et al., 2014).

3.2.3. *Impact of horizon discretization*

Based on the three-horizon model configuration, the second (15 cm) and third (40 cm) horizons were further subdivided at 1 cm intervals to

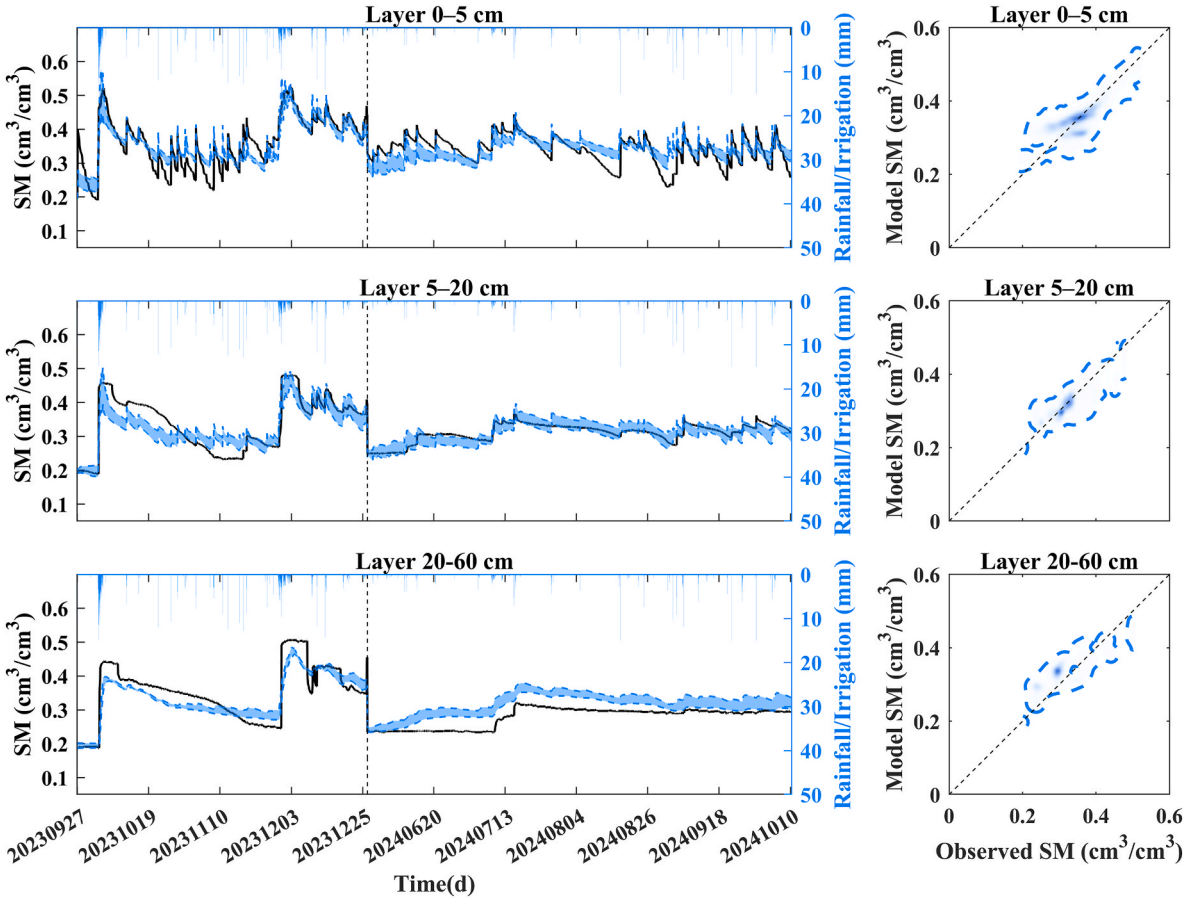

Fig. 12. Soil moisture simulations from the three-layer model R-FLX-ET_MUL_3_051540 with varying discretization levels within the second (15 cm) and third (40 cm) horizons. The blue shaded area in the time series plot represents the range of all simulation results, while the blue line in the scatter plot encloses all simulation ensembles. (For interpretation of the references to colour in this figure legend, the reader is referred to the Web version of this article.)

examine the influence of vertical discretization on soil moisture simulation accuracy, while the near-surface horizon was fixed at 5 cm thickness, aligned with UAV-based observations. The resulting simulations are shown in Fig. 12, where the blue shaded area in the timeseries plot encompassed the range of all simulation results, and the blue line in the scatter plot enveloped all the simulation ensembles across the full simulation period. Model simulations in the near-surface layer were relatively widespread during rainfall/irrigation events, highlighting the sensitivity of near-surface soil moisture to vertical discretization. However, the model ensemble still captured the overall temporal dynamics well. In the middle 5–20 cm layer, the spread of simulation results narrowed compared to the near-surface layer, with the model consistently capturing the observed wetting and drying cycles. The blue shaded area was narrowest in the deepest horizon (20–60 cm), where the simulation ensemble closely followed the in-situ data with minimal spread. This trend was also evident in the right-hand scatter plots, where the cloud of simulation aligned progressively more tightly with the 1:1 line from the near-surface to deeper layers. These results suggested that vertical discretization had a more pronounced influence on near-surface soil moisture simulation due to rapid near-surface distribution. In contrast, subsurface layers benefited from smoother dynamics and were less sensitive to the exact layer configuration. Overall, the analysis demonstrated that the impact of horizon discretization on the model accuracy is subtle, consistent with previous findings that soil moisture simulations are generally more sensitive to process representation and parameterization than to vertical resolution (Clark et al., 2015; He et al., 2021).

3.3. Impact of root zone depth definitions

To assess the influence of root zone depth on the model accuracy, root zone depth was set to different depths ranging from 15 cm to 40 cm, consistent with the locations of soil moisture sensors, and parameters calibrated separately for each configuration. As soil moisture models with additional horizons and discretization did not yield substantial improvements, the two-layer soil moisture model R-FLX-ET was applied for this analysis. Fig. 13 presents the R and RMSE between modeled and observed RZSM for the corresponding depths. Across all tested depths, the R maintained around 0.90 and RMSE was around 0.02 cm^3/cm^3 for the calibration period. While results deteriorated slightly in the validation period, the two-layer soil moisture model R-FLX-ET could still provide a reliable performance for estimating RZSM, achieving $R \approx 0.8$ and RMSE slightly over 0.04 cm^3/cm^3. This demonstrated that the soil moisture model R-FLX-ET was robust to the choice of root zone depth and can be reliably applied regardless of the defined root zone depth, demonstrating its flexibility and usefulness for application to precision irrigation under different crop types.

4. Conclusion

To improve root zone soil moisture (RZSM) estimation for supporting precision irrigation scheduling, this study explored a set of alternate conceptual soil moisture models based on an initial single-layer bucket model framework, with the aim of identifying a suitable model structure, which requires at least two soil layers while maintains minimal complexity, for coupling with UAV-derived near-surface soil moisture observations. Key water balance components, including vertical soil moisture redistribution, evapotranspiration, deep drainage and infiltration were progressively refined to assess their contribution to model accuracy. Multi-layer models were then developed from the initial two-layer model configuration found to give the best results, based on a balance between accuracy and simplicity. The key conclusions of the analysis are as follows:

(1) Soil moisture redistribution and evapotranspiration are the two most critical components for accurate soil moisture estimation. A two-layer model configuration (R-FLX-ET), incorporating vertical redistribution based on the Buckingham-Darcy equation and a revised evapotranspiration scheme was identified as the optimal model structure. It achieved R values up to 0.9600 for the root zone and 0.8891 for the near-surface layer when using hourly meteorological forcing, with RMSE values below 0.03 cm^3/cm^3 at a soil moisture monitoring station where systematic evaluations of alternate two-layer model structures were conducted. The R-FLX-ET model was superior to both the SL (NSE = 0.5033 for hourly) and Aqua Crop (NSE = 0.7836 for daily RZSM estimations) models. It also demonstrated strong numerical stability under different temporal solution schemes, including different temporal resolution of the meteorological datasets, explicit and implicit time-stepping schemes, as well as variable time-stepping approaches. Hourly meteorological forcing data was found to give better performance, especially for capturing the near-surface soil moisture dynamics, and so is recommended when utilizing UAV-based near-surface moisture to improve RZSM estimations. The reliability of R-FLX-ET was further confirmed across other soil moisture monitoring stations with both irrigated and rainfed regimes. Moreover, varying the root zone depth definitions from 15 to 60 cm did not influence the model robustness, confirming its applicability to alternative crops with diverse rooting depths.

(2) Multi-layer models based on R-FLX-ET provided only marginal improvements to the two-layer model. While additional horizons allowed a more detailed discretization of soil moisture dynamics, improvements were limited to intermediate layers and did not substantially improve the estimation of average soil moisture across the full soil profile. Soil moisture estimations based on

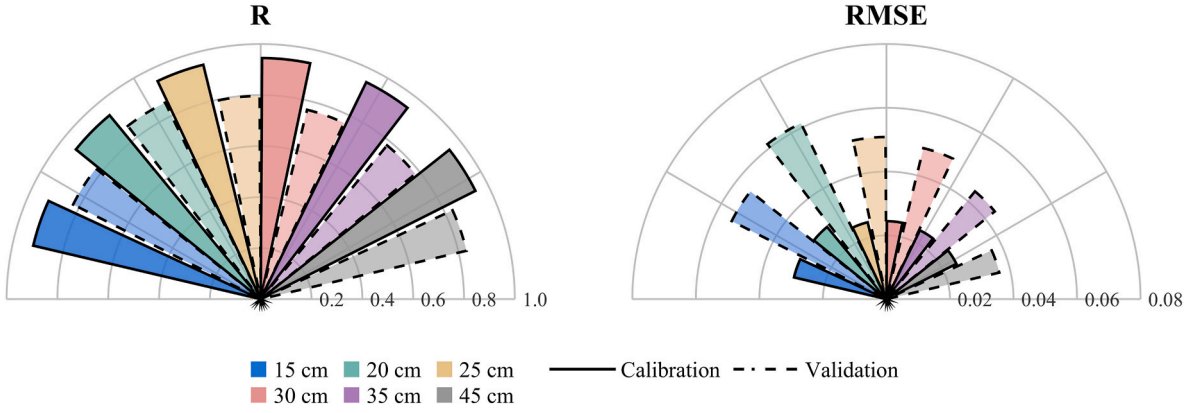

Fig. 13. Correlation coefficient (R) and root mean square error (RMSE) between simulated and observed root-zone soil moisture (RZSM) for different definitions of root-zone depth.

finer discretization performed comparably without giving further improvement. This indicated that the two-layer R-FLX-ET model already provided robust and reliable RZSM estimations without the need for additional complexity.

Overall, this study demonstrated that a parsimonious two-layer soil moisture model (R-FLX-ET) that explicitly accounts for soil moisture redistribution and evapotranspiration from different soil layers is sufficient for accurate simulation of both near-surface and root zone soil moisture. R-FLX-ET offers a favorable trade-off between structural simplicity, computational efficiency, and simulation accuracy, and thus provides a practical foundation for future studies coupling UAV-derived near-surface moisture to further improve RZSM mapping in support of precision irrigation applications.

CRediT authorship contribution statement

Meng Cao: Conceptualization, Formal analysis, Methodology, Writing – original draft. **Jeffrey P. Walker:** Methodology, Supervision, Visualization, Writing – review & editing. **Xiaoling Wu:** Resources, Supervision, Writing – review & editing. **Mostafa Rahimi Jamnani:** Software. **John D. Bussell:** Resources, Writing – review & editing. **Ivor Gaylard:** Funding acquisition, Resources. **James Hills:** Funding acquisition, Writing – review & editing.

Declaration of competing interest

The authors declare that they have no known competing financial interests or personal relationships that could have appeared to influence the work reported in this paper.

Acknowledgements

This work was supported by the Australian Research Council Linkage Grant LP210301314: Smart Irrigation: Integrating UAV Soil Moisture Maps & Variable Rate Sprays. The authors wish to thank Pascal Mater and Mahala Ebery for their help with maintenance of the experimental equipment and site. The authors acknowledge the research teams and volunteers participating in the fieldwork.

Appendix A. Supplementary data

Supplementary data to this article can be found online at https://doi.org/10.1016/j.envsoft.2026.107065.

Data availability

All the soil moisture models applied in this manuscript and the related dataset are freely available at: https://github.com/mengcao-prog/R-FLX-soil-moisture-model.

References

Aboitiz, M., Labadie, J.W., Heermann, D.F., 1986. Stochastic soil-moisture estimation and forecasting for irrigated fields. Water Resour. Res. 22, 180–190.
Ahmadi, S., Alizadeh, H., Mojaradi, B., 2022. Land surface temperature assimilation into a soil moisture-temperature model for retrieving farm-scale root zone soil moisture. Geoderma 421.
Allen, R.G., Pruitt, W.O., Wright, J.L., Howell, T.A., Ventura, F., Snyder, R., Itenfisu, D., Steduto, P., Berengena, J., Yrisarry, J.B., Smith, M., Pereira, L.S., Raes, D., Perrier, A., Alves, I., Walter, I., Elliott, R., 2006. A recommendation on standardized surface resistance for hourly calculation of reference ETO by the FAO56 Penman-Monteith method. Agric. Water Manag. 81, 1–22.
Allen, R.G., Smith, M., Pereira, L.S., Pruitt, W.O., 1996. Proposed revision to the FAO procedure for estimating crop water requirements. In: 2nd International Symposium on Irrigation of Horticultural Crops, pp. 17–33. Khania, Greece.
Baldwin, D., Manfreda, S., Keller, K., Smithwick, E.A.H., 2017. Predicting root zone soil moisture with soil properties and satellite near-surface moisture data across the conterminous United States. J. Hydrol. 546, 393–404.
Bandara, R., Walker, J.P., Rüdiger, C., 2013. Towards soil property retrieval from space: a one-dimensional twin-experiment. J. Hydrol. 497, 198–207.
Ben Touhami, H., Lardy, R., Bellocchi, G., Ben Touhami, H., Lardy, R., Barra, V., Bellocchi, G., 2013. Screening parameters in the pasture simulation model using the morris method. Ecol. Model. 266, 42–57.
Bogena, H.R., Huisman, J.A., Oberdörster, C., Vereecken, H., 2007. Evaluation of a low-cost soil water content sensor for wireless network applications. J. Hydrol. 344, 32–42.
Campolongo, F., Cariboni, J., Saltelli, A., 2007. An effective screening design for sensitivity analysis of large models. Environ. Model. Software 22, 1509–1518.
Campoy, A., Ducharne, A., Cheruy, F., Hourdin, F., Polcher, J., Dupont, J.C., 2013. Response of land surface fluxes and precipitation to different soil bottom hydrological conditions in a general circulation model. J. Geophys. Res. Atmos. 118, 10725–10739.
Chen, X.D., Liang, X., Xia, J., She, D.X., 2018. Impact of lower boundary condition of richards' equation on water, energy, and soil carbon based on coupling land surface and biogeochemical models. Pedosphere 28, 497–510.
Clark, M.P., Fan, Y., Lawrence, D.M., Adam, J.C., Bolster, D., Gochis, D.J., Hooper, R.P., Kumar, M., Leung, L.R., Mackay, D.S., Maxwell, R.M., Shen, C.P., Swenson, S.C., Zeng, X.B., 2015. Improving the representation of hydrologic processes in Earth system models. Water Resour. Res. 51, 5929–5956.
Demaria, E.M., Nijssen, B., Wagener, T., 2007. Monte carlo sensitivity analysis of land surface parameters using the variable infiltration capacity model. J. Geophys. Res. Atmos. 112.
Dong, J.Z., Dirmeyer, P.A., Lei, F.N., Anderson, M.C., Holmes, T.R.H., Hain, C., Crow, W. T., 2020. Soil evaporation stress determines soil moisture-evapotranspiration coupling strength in land surface modeling. Geophys. Res. Lett. 47.
Duan, Q.Y., Gupta, V.K., Sorooshian, S., 1993. Shuffled complex evolution approach for effective and efficient global minimization. J. Optim. Theor. Appl. 76, 501–521.
Ducoudre, N.I., Laval, K., Perrier, A., 1993. Sechiba, a new set of parameterizations of the hydrologic exchanges at the land–atmosphere interface within the lmd atmospheric general-circulation model. J. Clim. 6, 248–273.
Evett, S.R., Tolk, J.A., Howell, T.A., 2006. Soil profile water content determination: sensor accuracy, axial response, calibration, temperature dependence, and precision. Vadose Zone J. 5, 894–907.
Feki, M., Ravazzani, G., Ceppi, A., Milleo, G., Mancini, M., 2018. Impact of infiltration process modeling on soil water content simulations for irrigation management. Water 10.
Filippucci, P., Tarpanelli, A., Brocca, L., Filippucci, P., Tarpanelli, A., Massari, C., Serafini, A., Strati, V., Alberi, M., Raptis, K.G.C., Mantovani, F., Brocca, L., 2020. Soil moisture as a potential variable for tracking and quantifying irrigation: a case study with proximal gamma-ray spectroscopy data. Adv. Water Resour. 136, 103502.
Franchini, M., 1996. Use of a genetic algorithm combined with a local search method for the automatic calibration of conceptual rainfall-runoff models. Hydrol. Sci. J. 41, 21–39.
Geng, Y.J., Leng, P., Kasim, A.A., Song, X.N., Li, Z.L., 2025. Soil moisture estimation from satellite-derived temporal signals in the thermal domain with an improved parameterization scheme. J. Hydrol. 662.
Guswa, A.J., Celia, M.A., Rodriguez-Iturbe, I., 2002. Models of soil moisture dynamics in ecohydrology: a comparative study. Water Resour. Res. 38.
Han, S.J., Tian, F.Q., Gao, L., 2020. Current status and recent trend of irrigation water use in China. Irrig. Drain. 69, 25–35.
He, J.H., Hantush, M.M., Isik, S., He, J., Hantush, M.M., Kalin, L., Rezaeianzadeh, M., Isik, S., 2021. A two-layer numerical model of soil moisture dynamics: model development. J. Hydrol. 602, 126797.
Hirschi, M., Mueller, B., Dorigo, W., Seneviratne, S.I., 2014. Using remotely sensed soil moisture for land-atmosphere coupling diagnostics: the role of surface vs. root-zone soil moisture variability. Rem. Sens. Environ. 154, 246–252.
Horton, R.E., 1933. The role of infiltration in the hydrologic cycle. Trans. Am. Geophys. Union 14, 446–460.
Hu, W., Chau, H.W., Qiu, W.W., Si, B.C., 2017. Environmental controls on the spatial variability of soil water dynamics in a small watershed. J. Hydrol. 551, 47–55.
Jarvis, N., Larsbo, M., Lewan, E., Garré, S., 2022. Improved descriptions of soil hydrology in crop models: the elephant in the room? Agric. Syst. 202.
Jones, H.G., 2004. Irrigation scheduling: advantages and pitfalls of plant-based methods. J. Exp. Bot. 55, 2427–2436.
Kashyap, B., Kumar, R., 2021. Sensing methodologies in agriculture for soil moisture and nutrient monitoring. IEEE Access 9, 14095–14121.
Kennedy, J., Eberhart, R., 1995. Particle swarm optimization. In: 1995 IEEE International Conference on Neural Networks (ICNN 95). Univ W Austraia, Perth, Australia, pp. 1942–1948. Ieee, Ieee, Ieee, & Ieee.
Khakbaz, B., Imam, B., Hsu, K., Sorooshian, S., 2012. From lumped to distributed via semi-distributed: calibration strategies for semi-distributed hydrologic models. J. Hydrol. 418, 61–77.
Khandan, R., Wigneron, J.P., Bonafoni, S., Biazar, A.P., Gholamnia, M., 2022. Assimilation of satellite-derived soil moisture and brightness temperature in land surface models: a review. Remote Sens. 14.
Kumar, R., Shankar, V., Jat, M.K., 2013. Soil moisture dynamics modeling considering multi-layer root zone. Water Sci. Technol. 67, 1778–1785.
Li, L., Li, X.F., Zheng, X.M., Ju, H.Y., Li, X.J., Jiang, T., Wan, X.K., 2025. Estimating maize root zone soil moisture by assimilating high spatiotemporal resolution optical and radar remote sensing into the WOFOST-HYDRUS coupled model. J. Hydrol. 651.
MacBean, N., Scott, R.L., Biederman, J.A., Ottlé, C., Vuichard, N., Ducharne, A., Kolb, T., Dore, S., Litvak, M., Moore, D.J.P., 2020. Testing water fluxes and storage from two hydrology configurations within the ORCHIDEE land surface model across US semi-arid sites. Hydrol. Earth Syst. Sci. 24, 5203–5230.

McDonald, N., Luke, J., Cosby, A., 2024. Non-technical skills needed for the current and next-generation agricultural workforce. Agriculture-Basel 14.
McKay, R.C., Boschat, G., Rudeva, I., Pepler, A., Purich, A., Dowdy, A., Hope, P., Gillett, Z.E., Rauniyar, S., 2023. Can southern Australian rainfall decline be explained? A review of possible drivers. Wiley Interdiscip. Rev. Clim. Change 14.
Meng, C.L., Jin, H.D., Zhang, W.L., Meng, C., Jin, H., Zhang, W., 2023. Lateral terrestrial water flow schemes for the Noah-MP land surface model on both natural and urban land surfaces. J. Hydrol. 620, 129410.
Miralles, D.G., Bonte, O., Koppa, A., Baez-Villanueva, O.M., Tronquo, E., Zhong, F., Beck, H.E., Hulsman, P., Dorigo, W., Verhoest, N.E.C., Haghdoost, S., 2025. GLEAM4: Global Land Evaporation and Soil Moisture Dataset at 0.1 Resolution from 1980 to near Present, 12. Scientific Data.
Morris, M.D., 1991. Factorial sampling plans for preliminary computational experiments. Technometrics 33, 161–174.
Ojha, N., Mahmoodi, A., Mialon, A., Richaume, P., Ferrant, S., Kerr, Y.H., 2024. Assessment of SMOS root zone soil moisture: a comparative study using SMAP, ERA5, and GLDAS. IEEE Access 12, 76121–76132.
Pablos, M., González-Zamora, A., Sánchez, N., Martínez-Fernández, J., 2018. Assessment of root zone soil moisture estimations from SMAP, SMOS and MODIS observations. Remote Sens. 10.
Pan, F.F., Nieswiadomy, M., Qian, S., 2015. Application of a soil moisture diagnostic equation for estimating root-zone soil moisture in arid and semi-arid regions. J. Hydrol. 524, 296–310.
Parrens, M., Mahfouf, J.F., Barbu, A.L., Calvet, J.C., 2014. Assimilation of surface soil moisture into a multilayer soil model: design and evaluation at local scale. Hydrol. Earth Syst. Sci. 18, 673–689.
Pereira, L.S., Allen, R.G., Smith, M., Raes, D., 2015a. Crop evapotranspiration estimation with FAO56: past and future. Agric. Water Manag. 147, 4–20.
Pereira, L.S., Paredes, P., Rodrigues, G.C., Neves, M., 2015b. Modeling malt barley water use and evapotranspiration partitioning in two contrasting rainfall years. Assessing aqua crop and SIMDualKc models. Agric. Water Manag. 159, 239–254.
Pinheiro, A.G., Alves, C.P., de Souza, C.A.A., Araújo Jr., G.D., Jardim, A., de Morais, J.E. F., de Souza, L.S.B., Lopes, D.D., Neto, A.J.S., Montenegro, A.A.D., Gomes, J.E.A., da Silva, T.G.F., 2024. Calibration and validation of the AquaCrop model for production arrangements of forage cactus and grass in a semi-arid environment. Ecol. Model. 488.
Qi, J.Y., Zhang, X.S., McCarty, G.W., Sadeghi, A.M., Cosh, M.H., Zeng, X.B., Gao, F., Daughtry, C.S.T., Huang, C., Lang, M.W., Arnold, J.G., 2018. Assessing the performance of a physically-based soil moisture module integrated within the soil and water assessment tool. Environ. Model. Software 109, 329–341.
Raes, D., Steduto, P., Hsiao, T.C., Fereres, E., 2009. AquaCrop-The FAO crop model to simulate yield response to water: II. Main algorithms and software description. Agron. J. 101, 438–447.
Rauniyar, S.P., Power, S.B., 2023. Past and future rainfall change in sub-regions of Victoria, Australia. Clim. Change 176.
Rekika, D., Caron, J., Rancourt, G.T., Lafond, J.A., Gumiere, S.J., Jenni, S., Gosselin, A., 2014. Optimal irrigation for onion and celery production and spinach seed germination in histosols. Agron. J. 106, 981–994.
Romano, N., Palladino, M., Chirico, G.B., 2011. Parameterization of a bucket model for soil-vegetation-atmosphere modeling under seasonal climatic regimes. Hydrol. Earth Syst. Sci. 15, 3877–3893.
Rouf, T., Girotto, M., Paul, H.C., Maggioni, V., 2021. Assimilating satellite-based soil moisture observations in a land surface model: the effect of spatial resolution. J. Hydrol. X 13.
Saab, M.T.A., Todorovic, M., Albrizio, R., 2015. Comparing Aqua Crop and CropSyst models in simulating barley growth and yield under different water and nitrogen regimes. Does calibration year influence the performance of crop growth models? Agric. Water Manag. 147, 21–33.
Sahaar, S.A., Niemann, J.D., Sahaar, S.A., Niemann, J.D., 2020. Impact of regional characteristics on the estimation of root-zone soil moisture from the evaporative index or evaporative fraction. Agric. Water Manag. 238, 106225.
Sahoo, S.R., Liu, J.F., 2022. Adaptive model reduction and state estimation of agro-hydrological systems. Comput. Electron. Agric. 195.
Saltelli, A., Annoni, P., Azzini, I., Campolongo, F., Ratto, M., Tarantola, S., 2010. Variance based sensitivity analysis of model output. Design and estimator for the total sensitivity index. Comput. Phys. Commun. 181, 259–270.
Scanlon, B.R., Faunt, C.C., Longuevergne, L., Reedy, R.C., Alley, W.M., McGuire, V.L., McMahon, P.B., 2012. Groundwater depletion and sustainability of irrigation in the US high plains and central valley. Proc. Natl. Acad. Sci. U. S. A 109, 9320–9325.
Scollo, S., Tarantola, S., Bonadonna, C., Coltelli, M., Saltelli, A., 2008. Sensitivity analysis and uncertainty estimation for tephra dispersal models. J. Geophys. Res. Solid Earth 113.
Seneviratne, S.I., Nicholls, N., Easterling, D., Goodess, C.M., Kanae, S., Kossin, J., Luo, Y. L., Marengo, J., McInnes, K., Rahimi, M., Reichstein, M., Sorteberg, A., Vera, C., Zhang, X.B., Rusticucci, M., Semenov, V., Alexander, L.V., Allen, S., Benito, G., Cavazos, T., Clague, J., Conway, D., Della-Marta, P.M., Gerber, M., Gong, S.L., Goswami, B.N., Hemer, M., Huggel, C., van den Hurk, B., Kharin, V.V., Kitoh, A., Tank, A., Li, G.L., Mason, S., McGuire, W., van Oldenborgh, G.J., Orlowsky, B., Smith, S., Thiaw, W., Velegrakis, A., Yiou, P., Zhang, T.J., Zhou, T.J., Zwiers, F.W., Intergov Panel Clim, C., 2012. Changes in climate extremes and their impacts on the natural physical environment. In: Managing the Risks of Extreme Events and Disasters to Advance Climate Change Adaptation, pp. 109–230.
State Government of Victoria, M., Australia, 2024. Victorian Department of Energy, Environment and Climate Action, 2024. *Gippsland Climate Projections 2024*.
Steduto, P., Hsiao, T.C., Raes, D., Fereres, E., 2009. AquaCrop-The FAO crop model to simulate yield response to water: I. Concepts and underlying principles. Agron. J. 101, 426–437.
Tang, X.Y., Tang, D.S., Zhang, F.L., Tang, X., Tang, D., Zhang, F., 2024. A framework for algorithmic improvement to mitigate the effects of equifinality in the calibration of high-dimensional parameters for hydrological models. Water Resour. Manag. 38, 251–267.
Techen, A.K., Helming, K., Brüggemann, N., Veldkamp, E., Reinhold-Hurek, B., Lorenz, M., Bartke, S., Heinrich, U., Amelung, W., Augustin, K., Boy, J., Corre, M., Duttman, R., Gebbers, R., Gentsch, N., Grosch, R., Guggenberger, G., Kern, J., Kiese, R., Kuhwald, M., Leinweber, P., Schloter, M., Wiesmeier, M., Winkelmann, T., Vogel, H.J., 2020. Soil research challenges in response to emerging agricultural soil management practices. In: Sparks, D.L. (Ed.), Advances in Agronomy, 161, pp. 179–240.
Tsiros, J.X., Elmaloglou, S., Ambrose, R.B., 1998. A comparative study of two methods for modeling soil water regime in agricultural fields. Water Resour. Manag. 12, 285–293.
van Dam, J.C., Feddes, R.A., 2000. Numerical simulation of infiltration, evaporation and shallow groundwater levels with the richards equation. J. Hydrol. 233, 72–85.
Vangenuchten, M.T., 1980. A closed-form equation for predicting the hydraulic conductivity of unsaturated soils. Soil Sci. Soc. Am. J. 44, 892–898.
Vereecken, H., Schnepf, A., Hopmans, J.W., Javaux, M., Or, D., Roose, D.O.T., Vanderborght, J., Young, M.H., Amelung, W., Aitkenhead, M., Allison, S.D., Assouline, S., Baveye, P., Berli, M., Brüggemann, N., Finke, P., Flury, M., Gaiser, T., Govers, G., Ghezzehei, T., Hallett, P., Franssen, H.J.H., Heppell, J., Horn, R., Huisman, J.A., Jacques, D., Jonard, F., Kollet, S., Lafolie, F., Lamorski, K., Leitner, D., McBratney, A., Minasny, B., Montzka, C., Nowak, W., Pachepsky, Y., Padarian, J., Romano, N., Roth, K., Rothfuss, Y., Rowe, E.C., Schwen, A., Simunek, J., Tiktak, A., Van Dam, J., van der Zee, S., Vogel, H.J., Vrugt, J.A., Wöhling, T., Young, I.M., 2016. Modeling soil processes: review, key challenges, and new perspectives. Vadose Zone J. 15.
Vianna, M.D., Metselaar, K., van Lier, Q.D., Gaiser, T., Marin, F.R., 2024. The importance of model structure and soil data detail on the simulations of crop growth and water use: a case study for sugarcane. Agric. Water Manag. 301.
Vrugt, J.A., Gupta, H.V., Bouten, W., Sorooshian, S., 2003. A shuffled complex evolution metropolis algorithm for optimization and uncertainty assessment of hydrologic model parameters. Water Resour. Res. 39.
Walker, J.P., Willgoose, G.R., Kalma, J.D., 2001a. One-dimensional soil moisture profile retrieval by assimilation of near-surface measurements: a simplified soil moisture model and field application. J. Hydrometeorol. 2, 356–373.
Walker, J.P., Willgoose, G.R., Kalma, J.D., 2001b. One-dimensional soil moisture profile retrieval by assimilation of near-surface observations: a comparison of retrieval algorithms. Adv. Water Resour. 24, 631–650.
Wöhling, T., Vrugt, J.A., Barkle, G.F., 2008. Comparison of three multiobjective optimization algorithms for inverse modeling of vadose zone hydraulic properties. Soil Sci. Soc. Am. J. 72, 305–319.
Wigmore, O., Mark, B., McKenzie, J., Baraer, M., Lautz, L., 2019. Sub-metre mapping of surface soil moisture in proglacial valleys of the tropical andes using a multispectral unmanned aerial vehicle. Rem. Sens. Environ. 222, 104–118.
Wu, M., Gao, Y.Q., Liu, Y.P., Xu, L.S., Gao, L., 2025. Application and effect evaluation of different optimization algorithms in distributed hydrological model. J. Hydrol.: Reg. Stud. 58.
Wu, X.L., Walker, J.P., Wong, V., 2023. Proximal soil moisture sensing for real-time water delivery control: exploratory study over a potato farm. Agriculture-Basel 13.
Xu, C.Y., Qu, J.J., Hao, X.J., Cosh, M.H., Prueger, J.H., Zhu, Z.L., Gutenberg, L., 2018. Downscaling of surface soil moisture retrieval by combining MODIS/Landsat and in situ measurements. Remote Sens. 10.
Xu, L., Chen, N.C., Chen, Z.Q., Zhang, C., Yu, H.C., 2021a. Spatiotemporal forecasting in Earth system science: methods, uncertainties, predictability and future directions. Earth Sci. Rev. 222.
Xu, L., Chen, N.C., Yang, C., Zhang, C., Yu, H.C., 2021b. A parametric multivariate drought index for drought monitoring and assessment under climate change. Agric. For. Meteorol. 310.
Xu, L., Chen, N.C., Zhang, X., Moradkhani, H., Zhang, C., Hu, C.L., 2021c. In-situ and triple-collocation based evaluations of eight global root zone soil moisture products. Rem. Sens. Environ. 254.
Xu, L., Ye, Z.N., Dai, J., Li, Q., Hong, Y.T., Tao, Y., Yu, H.C., Zhang, C., Chen, Z.Q., Chen, N.C., 2025. Spatiotemporal seamless estimation of global surface soil moisture using triple collocation, machine learning, and data assimilation. IEEE Trans. Geosci. Rem. Sens. 63.
Yu, J.X., Zhang, X., Xu, L.L., Dong, J., Zhangzhong, L.L., 2021. A hybrid CNN-GRU model for predicting soil moisture in maize root zone. Agric. Water Manag. 245.
Zeng, X.B., Decker, M., 2009. Improving the numerical solution of soil moisture-based richards equation for land models with a deep or shallow water table. J. Hydrometeorol. 10, 308–319.
Zha, Y.Y., Yang, J.Z., Shi, L.S., Zha, Y., Yang, J., Yin, L., Zhang, Y., Zeng, W., Shi, L., 2017. A modified Picard iteration scheme for overcoming numerical difficulties of simulating infiltration into dry soil. J. Hydrol. 551, 56–69.
Zhang, M., Ge, Y., Wang, J.H., 2024. Integrating infiltration processes in hybrid downscaling methods to estimate sub-surface soil moisture. Ecol. Inform. 84.
Zhao, X., Miao, C.Y., Hu, J.L., Su, J.J., 2025. Improving land surface model accuracy in soil moisture simulations using parametric schemes and machine learning. J. Hydrol. 657.